Effect of CuO/MgO ratio on the drug delivery kinetics of $CuO-MgO-P_2O_5-SiO_2-CaO-ZnO$ glasses

M.Tech. Thesis

Submitted in the partial fulfillment of the requirements for the award of Degree of

MASTER OF TECHNOLOGY

in

MATERIALS SCIENCE AND METALLURGY

by

Rupinderjeet bains

(Roll No. 601502005)

Under the supervision of

Dr. O P Pandey

Department of School of Physics and Materials Science

Thapar University, Patiala, Punjab, India

July, 2017

Certificate

This is to certify that the thesis entitled **"Effect of CuO/MgO ratio on the drug delivery kinetics of CuO-MgO-P_2O_5-SiO_2-CaO-ZnO glasses"** is an authentic record of my own work carried out as requirements for the award of degree of Master of Technology in Materials and Mettalurgical Engineering from Thapar University, Patiala, Punjab, under the supervision of Dr. O P Pandey, Senior Professor and Dean (R & SP), School of Physics and Materials Science, Thapar University, Patiala.

Rupinderjeet

Dated: 14-7-17

Rupinderjeet Bains
(Roll. No. 601502005)

This is certified that the above statement made by student is correct to the best of my knowledge and belief.

Dr. O P Pandey
Senior Professor and Dean (R & SP)
School of Physics and Materials Science
Thapar University, Patiala

ii

Declaration

I hereby declare that the work being presented in the thesis report entitled "**Effect of CuO/MgO ration on the drug delivery kinetics of CuO-MgO-P_2O_5-SiO_2-CaO-ZnO glasses"** by me in the partial fulfillment of the requirements for the award of degree of Master of Technology in Materials Science and Metallurgy from Thapar University, Patiala, Punjab, is an authentic record of my work carried under the supervision of Dr. O P Pandey, Senior Professor and Dean R & SP, Department of School of Physics and Materials Science, Thapar University, Patiala. The matter presented in this thesis has not been submitted in any other University/ Institute for the award of any degree / diploma.

Dated: 14-07-2017

Rupinderjeet Bains

(Roll. No. 601502005)

Acknowledgement

At this momentous occasion of binding my thesis I would like to acknowledge the contribution of all those benevolent people, I have been blessed to associate with. Behind every student there stands number of people whose help and contribution makes things successful.

My first and foremost offering of thanks goes to the architect who shaped my dreams into reality, my guide and mentor **Dr. O.P. Pandey (Senior Professor and Dean R & SP, School of Physics and Materials Science)** Perseverance, exuberance, positive approaches are just some of the traits he imprinted on my personality. He steered me through his journey through his invaluable advice, positive criticism, stimulating discussion and consistent encouragement. His meticulous attention towards my proceedings, his devoted time and his ideas has enabled me to make the project a success.

I would like to express my sincere thanks to **Dr. Manoj Kumar Sharma (HOD, School of Physics and Materials Science)** and the entire faculty members for their concern and suggestions during my project work and for providing me a friendly atmosphere throughout this research.

I would love to give special thanks to Senior Research Scientist **Dr. Gurbinder Kaur** for her valuable suggestion, strong motivation and constant encouragement during the course of the work. She has been very helpful in improving my thesis. I am grateful to her for sharing her time and expertise. Her comments and views were very helpful and insightful.

I would also love to thank **Mr. Aayush Gupta, Mr. Rameez Mir, Mr. Piyush Sharma,** and **Ms. Ruby Priya** for their constant support, help, suggestions and motivation whenever I required.

I am also thankful to my friends **Varun Singla, Harneet, Taranjot** for their support, help and encouragement.

Finally, I want to express my deepest gratitude to **GOD, My Parents** and **My brother,** to provide me support, help, big encouragement and lots of love.

Rupinderjeet Bains
(601502005)

Abstract

Copper and Magnesium based bioactive glasses with chemical composition (15-x)CuO-xMgO-10P_2O_5-60SiO_2-10CaO-5ZnO ($2.5 \leq x \leq 12.5$) were prepared by mixing raw materials in the organic form of cetyltrimethylammoniumbromide (CTAB), CaO, ZnO, SiO_2, P_2O_5, MgO and CuO by sol-gel technique. The pore size of the as prepared MBGs lies between 5.8 and 8.4nm whereas the surface area varies from 98.22 to 442.41 cm^2/g. The MBGs were loaded with the anticancerous, anti-inflammatory, antibiotic and antibacterial drugs, doxorubicin, Ibuprofen, amoxicillin and vancomycin, respectively. The increasing copper content influenced the bioactive as well as drug loading and release kinetics of diffferent drugs at different concentrations. In addition to this, the cytotoxicity assays were conducted for MG63 human osteosarcoma cell line. The prepared MBGs have high surface area and mesopore volume, high drug loading efficiency and controllable drug release.

Contents

List of Tables

List of Figures

CHAPTER 1
INTRODUCTION

1.1. General

In orthopedic surgery, bone graft infections are still a major medical problem and poses several major disadvantages such as prolonged antimicrobial treatment, implant failure, increased healthcare costs, extensive bone debridement as well as increased patient morbidity [1-2]. To address such problems, it is very important to develop and evaluate new biomaterials with enhanced bioactivity for controlled drug–delivery systems and bone regeneration application. One of the most emerging therapeutic concepts in orthopedic surgery is implantable drug-delivery systems for local release of antibiotics, antiestrogens, growth factors chemotherapeutic agents and anti-inflammatory drugs in bone tissue so as to cure malignancies like cancer and tumors [3]. We are now on entrance to new era, where target delivery of drug to a man's tumor tissue seems like an achievable goal, which would improve survival rate and quality of life for patients.

1.2. Tissue Engineering (TE)

Tissue engineering is an emerging muti-disciplinary field, involving biomaterials science, cell biology as well as medicine. Tissue engineering aims to induce new functional tissue using combinations of functional cells, growth factors and biomaterials as shown in fig 1.1 [4]. It has been emerging as a valid approach that eliminates the problem of shortage of donor organs and tissues available for transplantation [5]. Harvesting of stem cells or osteoblasts from the patient which are then cultured on a scaffold in vitro is one of the hypothesis for bone tissue engineering application. The TE bone/scaffold can then be implanted in the defect site and must undergo degradation at the same rate as the bone is regenerated [6-7]. Bioceramics such as calcium phosphates, hydroxyapatite (HA), bioactive glasses and composite materials combining bioactive inorganic materials with biodegradable polymers are some of the most attractive biomaterials for bone tissue engineering applications [8-9].

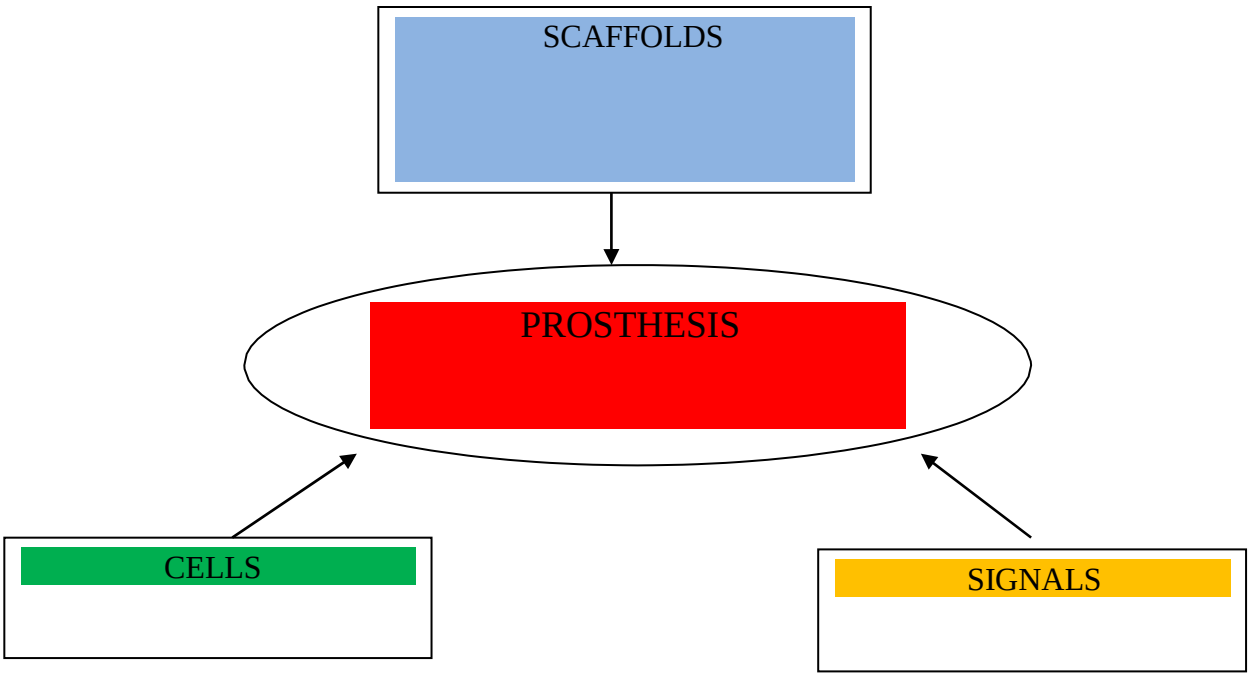

Fig 1.1: The tissue engineering triad [10].

1.3. Why tissue engineering?

The origin of tissue engineering is from the reconstructive surgery, in which the repair of damaged tissue is done through the direct transplantation of donor tissue. Since decade, the replacement of organs has been the matter of debate but the field of repairing and regenerating tissues in vivo, originated only about 20 years ago. The direct transplantation of organs involves many difficulties. Artificial implantation (autografts) or transplantation (allografts) for the repair of large bone defects is successful only for a limited time because of several disadvantages [11-12]. They are as follows:-

- Immune rejection or disease transmission from donor
- Blood loss and donor site morbidity
- Shortage of graft availability
- Lack of ability of living tissues to self-repair

Thus, tissue engineering provides a promising approach to overcome the limitations with traditional methods of direct transplantation, by repairing and regenerating the damaged tissues, instead of replacing them. Tissue engineering enhances the regenerative ability of the host body by mimicking the function of natural tissues.

1.4. Introduction to Bioactive glasses (BG)

Bioactive glass exhibits amorphous structure and is used in bone repair applications. In general sense, bioactive glasses may be defined as the glasses composed of SiO_2, Na_2O, CaO and P_2O_5 in specific proportion and are specifically designed to induce biological activity. When implanted into the body, it undergoes specific surface reactions and forms an HA-like layer. The proportion of components in bioactive glasses is different from the traditional sodalime glasses, whereas in case of bioactive glasses the amount of silica should be low (less than 60 mol%), high amount of sodium and calcium and higher calcium to phosphorous ratio, which make bioglass highly reactive to aqueous medium and bioactive. Highly Ca/P ratio promotes the formation of apatite crystals and helps to form bond with the bone. They have the ability to bond with both bone and soft tissue by the formation of HA layer and are known as class A category of bioactive materials [13-14]. BGs are fabricated by two methods: melt-quenching and sol-gel technique. The composition and synthesis route of various bioactive glasses are shown in table 1.1. Various imperative parameters for the bioactive glasses are as follows :-

- Avoiding any adverse effect on the cells
- Resorbability
- Biocompatibility
- Dissolution
- Excellent mechanical properties such as hardness and flexural strength.

Bioactive glasses are very promising materials for the fabrication of scaffolds because of their versatile properties, which can be properly designed depending on their composition. Lots of work has been done in the field of tissue engineering using different glass compositions, and some of them some are listed in table 1.1 [15-24].

Table 1.1: Compositions and synthesis techniques of typical bioactive glasses [15-24].

Glass Label	SiO_2	B_2O_3	P_2O_5	MgO	Na_2O	CaO	CuO	K_2O/ SrO/ CaF_2	ZnO	Method used	Wt%/ Mol%
45S5	46.1		2.6		24.4	26.9				Sol-gel	Mol%
13-93	53		4	5	6	20		12 K_2O		Melt-quench	Wt%
13-93 B1	34. 4	19.9	3.8	4.9	5.8	19.5		11.7 K_2O		Melt-quench	Wt%
13-93 B2 (D-Alk-B)	18	36	2	8	6	22		8 K_2O		Melt-quench	Wt%
13-93 B3		56.6	3.7	4.6	5.5	18.5		11.1 K_2O		Melt-quench	Wt%
SKC	50					44		6 K_2O		Melt-quench	Mol%
CEL2	45		3	7	15	26		4 K_2O		Melt-quench	Mol%
FaGC	50		6	3	7	18		7 K_2O/ 9 CaF_2		Melt-quench	Mol%
70S30C	70					30			4	Sol-gel	Mol%
SCNA	57				6	34		3 CaF_2		Melt-Quench	Mol%
G13	34.5		16.5	8.5		40		0.5 CaF_2		Melt-Quench	Wt%
BT110	0.4				0.1	0.1		0.2 SrO	0.2	Melt-quench	Mol%
BT111	0.4				0.2	0.1		0.2 SrO	0.1	Melt-quench	Mol%
BT112	0.4				0.3	0.1		0.2 SrO	0	Melt-quench	Mol%
BT113	0.4				0.1	0		0.3 SrO	0.2	Melt-quench	Mol%
BT114	0.4				0.2	0		0.3 SrO	0.1	Melt-quench	Mol%
BT115	0.4				0.3	0		0.3 SrO	0	Melt-quench	Mol%
HZ5	42.54		5.64		23.27	23.40			4.94	Melt-quench	Wt%
HZ10	40.44		5.39		22.08	22.02			10.05	Melt-quench	Wt%
HZ20	37.14		4.64		18.75	18.86			20.13	Melt-quench	Wt%
CP5	60	5	5			20			10	Sol-gel	Wt%
CP10	60	5	10			15			10	Sol-gel	Wt%
CP15	60	5	15			10			10	Sol-gel	Wt%
CP20	60	5	20			5			10	Sol-gel	Wt%
GCu2.5	60	5	10			22.5	2.5			Sol-gel	Mol%
GCu5	60	5	10			20	5			Sol-gel	Mol%
GCu7.5	60	5	10			17.5	7.5			Sol-gel	Mol%
GCu10	60	5	10			15	10			Sol-gel	Mol%
Cu8Zn2	60		10			20	8		2	Sol-gel	Mol%
Cu6Zn4	60		10			20	6		4	Sol-gel	Mol%
Cu4Zn6	60		10			20	4		6	Sol-gel	Mol%
Cu2Zn8	60		10			20	2		8	Sol-gel	Mol%
8Sr2Mg	60		10	2		20		8		Sol-gel	Mol%
6Sr4Mg	60		10	4		20		6		Sol-gel	Mol%
4Sr6Mg	60		10	6		20		4		Sol-gel	Mol%
2Sr8Mg	60		10	8		20		2		Sol-gel	Mol%

1.5. Bioactive glasses as drug carriers

Bioactive glasses are suitable and strong candidates for drug delivery as it fulfills the mandatory requirements for the delivery of biomolecules i.e. excellent biodegradability, osteoconductivity, bioresorbability and biocompatibility of the matrix, which helps in promoting crucial cell functions such as adhesion, proliferation and differentiation [25-26]. BGs loaded with specific therapeutic drugs (e.g., antibiotics) are locally delivered at the implantation site, hence promoting quick bone healing and osteogenesis [27-28]. The bioglass exhibits high bioactivity and it readily interacts with the soft tissues. Bioactive glasses have gained attention as bone substitute material (BSM), because they have tendency to build strong interface between tissue and material surface. Scaffolds based on inorganic materials are more interestingly developed because of the capability of scaffold to act as drug and biomolecule carrier vehicle. Drug delivery system also provides an advantage of local delivery of rapid flush of proteins and growth factors (without a carrier) on the target organ or infected area [29-30].

1.6. Mesoporous bioactive glasses (MBGs)

In last two decades, mesoporous materials have gained a lot of attraction. Mesoporous bioactive glasses (MBGs) exhibit a well ordered mesoporous structure with a pore size ranging from 2 to 50 nm. Mesoporous materials have applications in field of bone regeneration and drug delivery applications. MBGs are synthesized by a sol-gel technique by the incorporation of structure-directing agents and possess excellent bioactivity, cytocompatibilty and enhanced drug-delivery [31-32]. Mesoporous walls of MBGs contain different organic groups, which help in drug loading as well as releasing on the implant site through a local drug system and hence can solve the problem of osteomyelitis in bone reconstruction surgeries [33-34]. Mobil Composition of Matters (MCM)-41was the first mesoporous material used as drug delivery vehicle in 2001 [35]. Different structure- directing agents like cetyltrimethyl ammounium bromide (CTAB), F127, P123 etc influence the properties of BGs, i.e is, F127 produces a wormlike mesopore structure while two-dimensional hexagonal mesopore structure of pore-size 4-10 nm is obtained by using P123 into the glass structure. CTAB- contained BGs produce mesopore channel of pore size 2-3 nm. Generally, preparation of MBG using P123 or F127 is much more favorable as compared to CTAB [36].

1.7. Why mesoporous materials as drug delivery systems (DDSs)?

Osteomyelitis caused by bacteria infection is the main complication in conventional treatments such as wound drainage, implant removal and surgical debridement. Patient may suffer from extra surgeries because this is not one of the efficient approaches. Therefore, local drug release system into the implant site is an alternative approach to prevent/ treat peri-implant infections. High drug delivery efficiency, reduced toxicity and continuous action are some of the advantages of mesoporous materials. These materials with excellent bioactivity and efficient drug delivery can overcome the limitations of conventional bioactive glasses and pure mesopore SiO_2 [37]. Following features of mesoporous materials make it excellent candidates for controlled DDSs [3]. They are as follows:-

a) High pore volume
b) Optimal surface area for drug adsorption
c) An ordered pore network
d) A silanol-containing surface

1.8. Fabrication of mesoporous bioactive glasses (MBGs): Sol-gel technique

Silanol groups ($Si(OH)_4$) are formed when silicon alkoxide is hydrolysed. Sols are the colloidal particles (diameter in the range of 1–100 nm) dispersed in a liquid. A rigid network made up of interconnected pores and polymeric chains is known as gel. The gel is also formed by network formed from a group of colloidal particles. The first step of sol-gel process involves mixing of all the organometallic precursors and structure-assisting agent CTAB together. In the second step, liquid alkoxide precursors are hydrolyzed with de-ionized water, giving rise to silanol groups ($Si(OH)_4$). The next process is polycondensation where silica network (SiO_2) is formed and water is given out as a byproduct The hydrolysis and polycondensation work simultaneously and their kinetics is affected by various factors like pH, pressure, temperature, composition, alkoxide precursor, concentration of different ion species [38-39].

Hydrolysis:

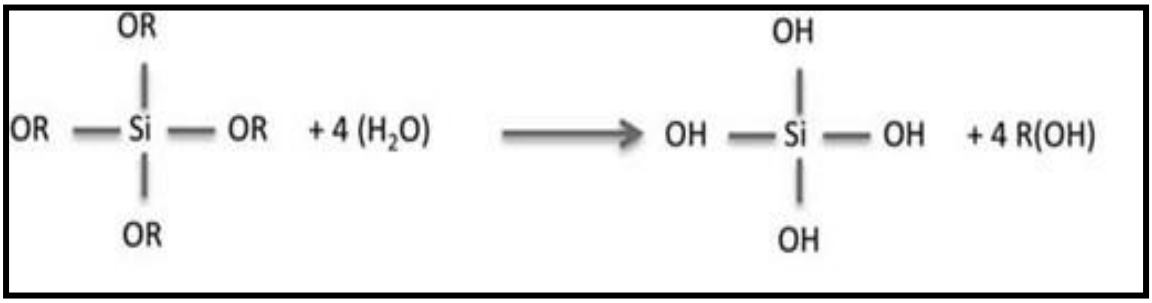

(1.1)

Condensation and Polymerization:

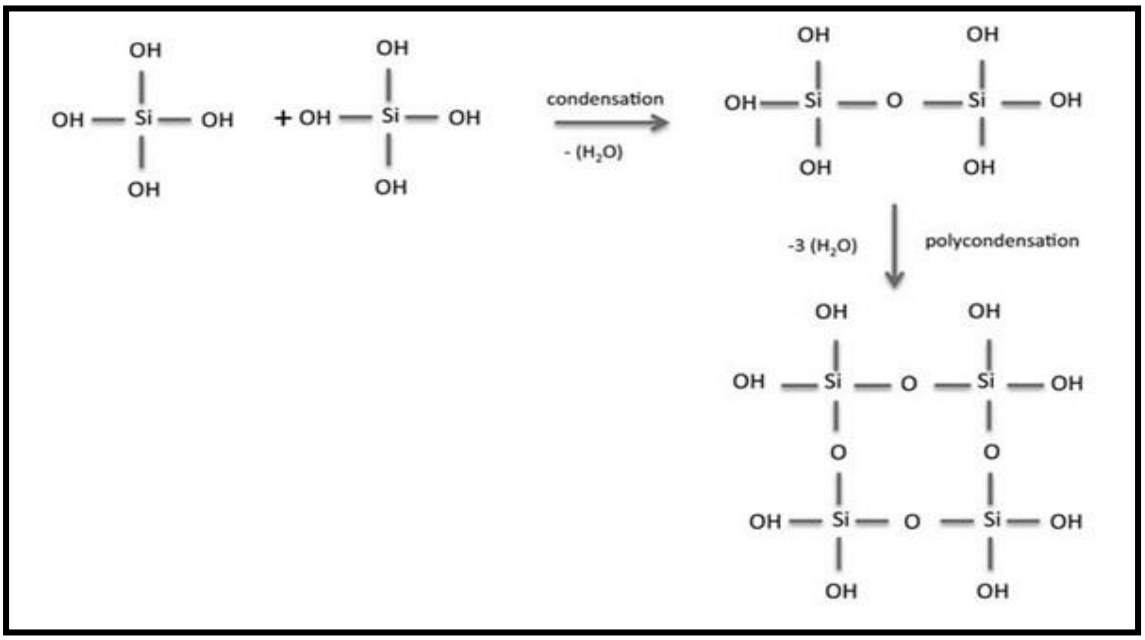

(1.2)

After the sol is formed, the process of gelation occurs where condensation and cross-linking of silica particles and other colloids takes place and a three-dimensional network is formed. An abrupt increase in the viscosity is observed during the gelation process. The point during which the gel behaves like an elastic solid is known as the gelation point (t_g) [40]. The next step is the aging of a gel where phase transformation, increase in strength as well as decrease in porosity of

as formed materials is observed [41]. In the last step, with the removal of pore liquid from interconnected rigid 3-D network, aged gel can be dried. After the silanol (Si-OH) removal/dehydration from within the pore network, a highly porous solid is formed [42]. The sol gel process is demonstrated in fig 1.2.

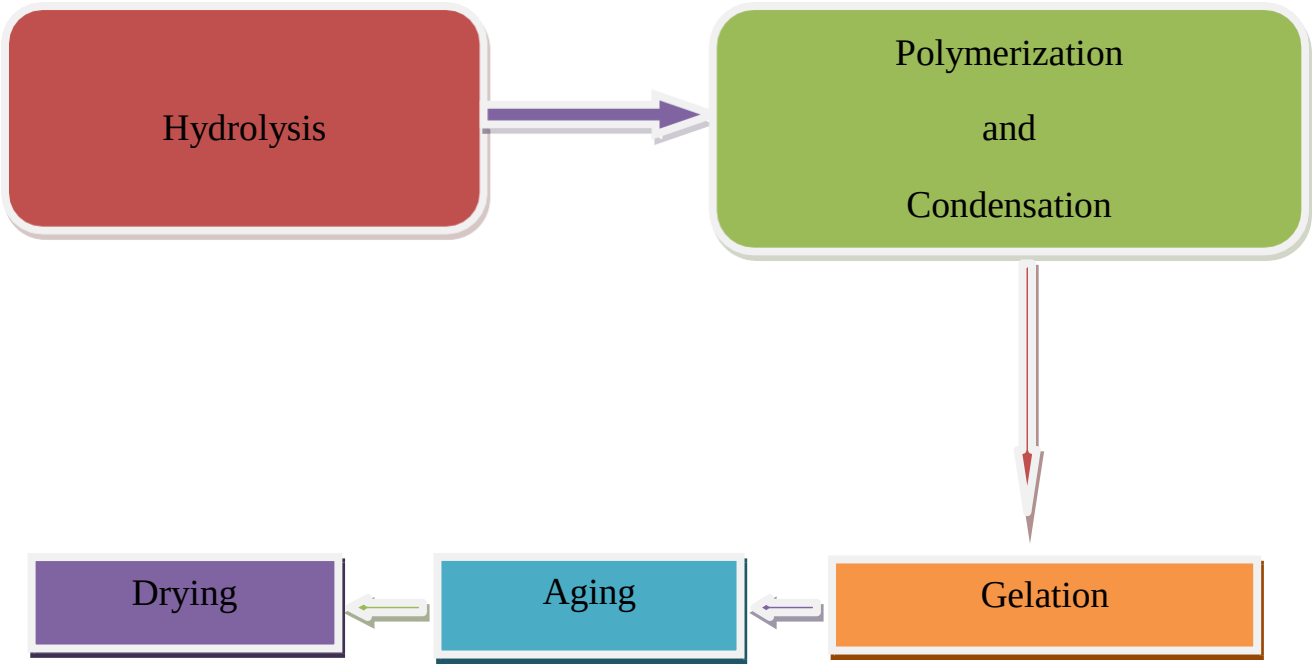

Fig 1.2: Sol-gel Process.

1.9. Functionalization of Mesoporous Drug-Delivery Systems

In drug delivery systems, loading and releasing of drug depend on the modification/ functionalization of the surface through organic groups. The drug release can be efficiently controlled by increasing the drug-surface interaction. The interaction between mesopore and drug is a surface phenomenon, which depends on two factors i.e. pore volume and insoluble porous networks of mesopores. The porewall structures of mesoporous glasses assist the confinement of drug molecules inside the cavities and physical adsorption without direct chemical bonding [43]. Consecutive loading of drugs in mesoporous materials will increase drug intermolecular interactions within pore voids which, in turn, will result in greater drug loading [38, 3, 44-45]. Common functional groups and high density of silanol groups on the surface of mesoporous silica together with several drugs is demonstrated in fig 1.3 [3].

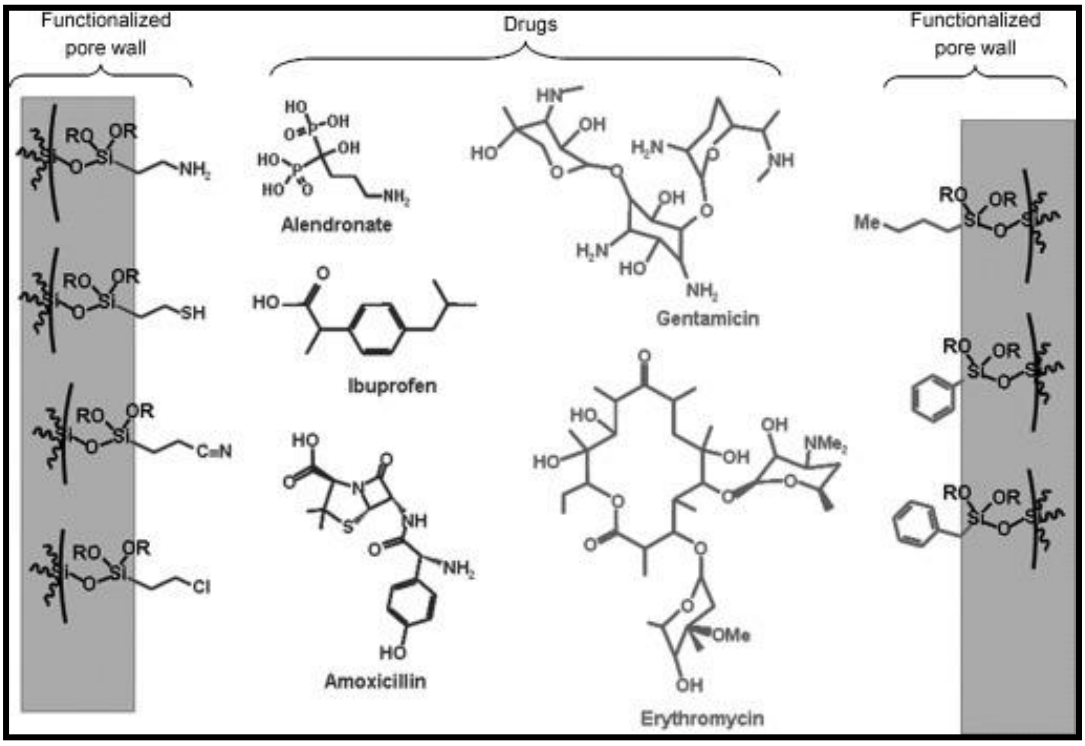

Fig 1.3: Structures of several drugs used in mesoporous silica [3].

1.10. Drug Candidates

For bone tissue engineering applications, antibiotics, anti-cancerous and anti-osteoporosis drugs have been found to play a vital role. In present work, antibacterial, anticancerous and anti-inflammatory drugs have been incorporated into MBGs. The particulars of the drugs are discussed in following sections:-

1.10.1. Vancomycin hydrochloride (VANCO)

Vancomycin hydrochloride (VANCO) ($C_{66}H_{75}Cl_2N_9O_{24}\cdot HCl$) is a peptide antibiotic drug having molecular weight of 1485.71 g/mol. It is used for curing the life-threatening infections caused by Gram-positive bacteria [46]. It is irritating to tissue and is always delivered through the intravenous route. It is a concentration-independent, time-dependent antibiotic with moderate postantibiotic effect (PAE). It is highly soluble in water and is used for the treatment of bone infections [47]. The molecular structure of VANCO is shown in fig 1.4.

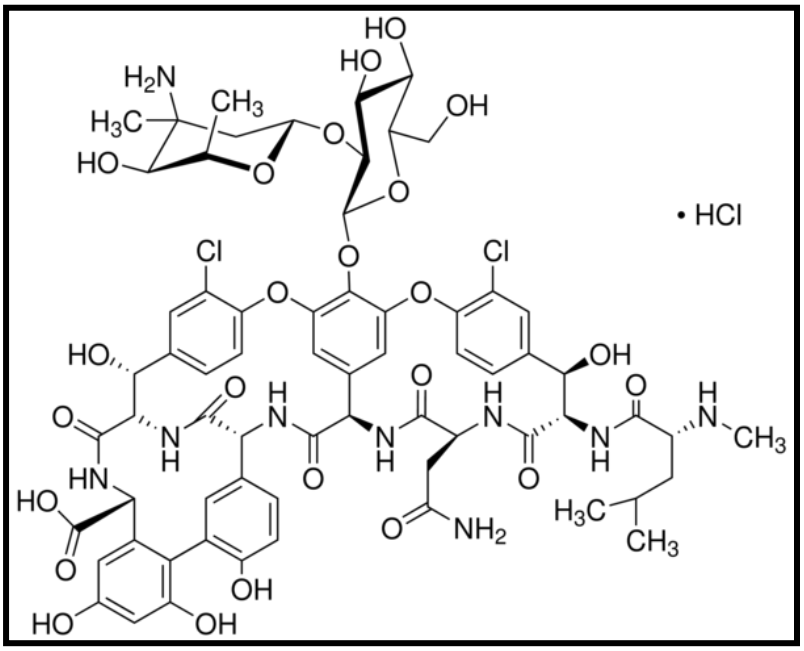

Fig 1.4. Molecular structure of Vancomycin hydrochloride [48].

1.10.2. Doxorubicin hydrochloride (DOX)

Doxorubicin hydrochloride (DOX) is an anti-cancerous drug comprising of 3-amino-2, 3, 4-trideoxy-L-fucosyl moiety ($C_{27}H_{29}NO_{11}$) as shown in fig 1.5. The drug is a nonselective class I anthracycline, which possess aglyconic and sugar moieties. To reduce the risk of toxicity, steady-state distribution of the DOX is essential [49].

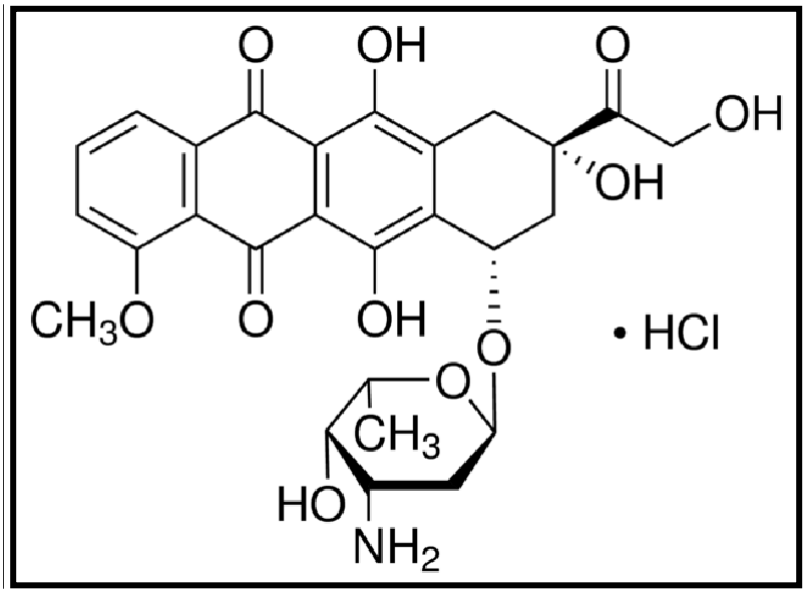

Fig 1.5. Chemical structure of Doxorubicin hydrochloride [50].

1.10.3. Ibuprofen (IBP)

Ibuprofen is a white crystalline and slightly waxy solid anti-inflammatory drug. Ibuprofen is particularly used when aspirin or acetaminophen does not give adequate pain relief. It is completely absorbed from the upper gastro-intestinal tract. It can also reduce dental pain [51]. Chemical structure of IBP is demonstrated in fig 1.6.

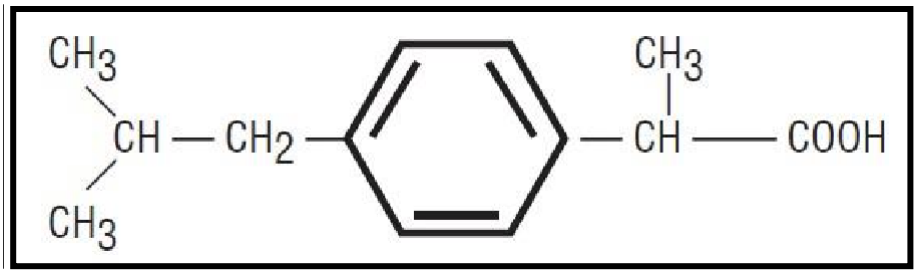

Fig.1.6. Chemical Structure of Ibuprofen [51].

1.11. Drug delivery profiles of mesoporous materials

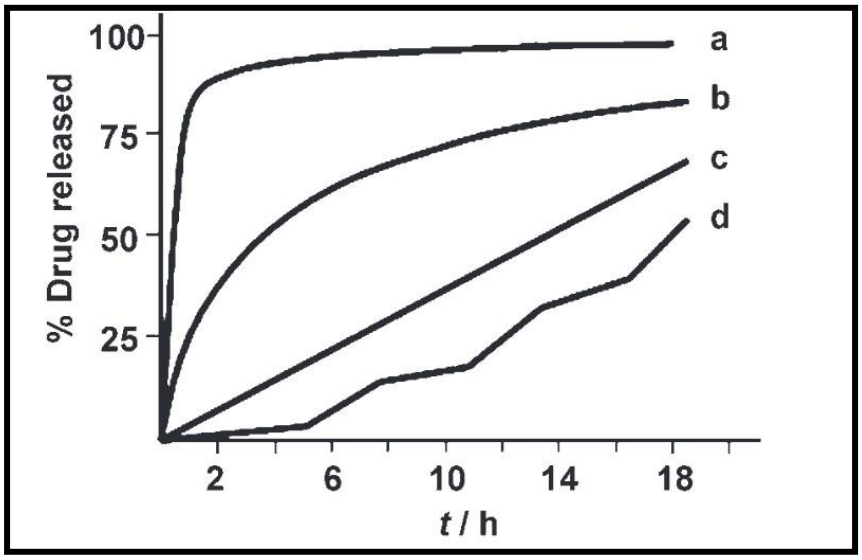

Fig.1.7. Common release profiles of mesoporous materials [3].

Fig 1.7 demonstrates release profiles for mesoporous materials. Profile **a** display a initial burst effect followed by a very slow drug release and is generally observed for nonfunctionalized matrices. This type of profile can be very useful for acute infections and inflammations, where a

high dose is required [35]. Profile **b** follows first order-kinetics with respect to drug concentration and is associated with diffusion process, for example, MCM-41 system. Profile **c** is highly desirable for long-term delivery systems as it follows zero-order kinetics. Here the release process is only time dependent. Amino-functionalized SBA-15 system is a good example of this profile. A more sophisticated stimulus-responsive system is represented by profile **d** where change in pH value, temperature, magnetic field etc can control the release rate [52].

1.12. Various Mesoporous Matrix- Drug systems

By tailoring the surface properties of mesoporous materials, effective control of drug release can be achieved.. Various matrix-drug systems along with adsorption conditions, structure-assisting agent and the amount of drug loaded into SiO_2-based mesoporous materials have been shown below in table 1.2.

Table 1.2: List of various drugs, adsorbtion conditions and maximum drug load adsorbed [35, 53-56].

Drug	Mesoporous matrix	Solvent	Max. load[%]	Surfactant
Ibuprofen	MCM-41_{12}	Hexane	23	C_{12}TAB
Ibuprofen	MCM-41_{16}	Hexane	34	C_{16} TAB
Gentamicin	PLGA-SiO_2	Water	22.4	Poly (D, L-lactic-co-glycolide)
Gentamicin	SBA-15	Water	20	
Erythromycin	MCM-48	Acetonitrile	28	
Erythromycin	LP-la3d	Acetonitrile	28	Large pore 3D cubic la3d mesoporous material
Aspirin	MCM-41	Water	15	
Aspirin	MCM-41-NH_2	Water	15	Organically modified with amino groups

1.13. Dosage in Mesoporous materials

Until now, we have studied that mesoporous materials can be excellent carriers for drugs, but however, we don't know how much drug should be implanted in mesoporous matrices to be delivered. Dosage i.e. the actual amount of drug that can be delivered to the targeted sites is a very important issue for drug-delivery systems. The dosages per impant are calculated from the maximum load percentages This amount of dosage depends upon some factors including patients characteristics, bioavailability and treatment duration. Table 1.3 lists mesoporous matrices proposed for DDS together with suitable drugs and daily dosage [3].

Table 1.3: A list of drugs and their daily dosage amounts [3].

Mesoporous matrix	Drug	Daily dose	Dosage (g)
SBA-15	Gentamicin	150-300 mg (intravenous)	2.0
SBA-15/PLGA	Gentamicin	150-300 mg (intravenous)	4.50
SBA-15	Erythromycin	1.5-3 g (oral)	3.4
SBA-15	Amoxiciline	1.5-2 g (oral)	2.50
SBA-15-NH_2	Alendronate	5-10 mg (oral)	2.0
MCM-41-NH_2	Alendronate	5-10 mg (oral)	2.5
MCM-41	Ibuprofen	0.9-1.2 g (oral)	7.0

1.14. Advantages of drug delivery system

In the past 30 years, controlled drug delivery technology has represented one of the most rapidly advancing research areas. The field is driven by the belief that controlled drug delivery will contribute significantly to human health. These drug delivery systems offer numerous advantages compared to conventional dosage forms [57-61]:-

- ♦ Increasing the efficacy of currently used drugs.
- ♦ Providing opportunities for the use of new agents currently precluded from clinical use due to challenges including low drug solubility and systemic toxicity.
- ♦ Reducing harmful side effects.
- ♦ Precise control of dose.
- ♦ Decreasing number of dosages.
- ♦ Improving patient compliance and convenience.

Due to excellent bio-compatibility, surface modification ability due to different functional groups and controlled drug delivery property, MBGs could play a significant role in controlled drug delivery systems. Hence, in the present investigation, Cu-Mg sol-gel glasses/ceramics are being aimed to synthesize as promising drug carriers and cytocompatible MTS assays. Moreover, a brief literature has been studied focusing on synthesis of various glass/glass-ceramic system for controlled drug delivery, which will be discussed in next chapter.

REFERENCES

[1] Zimmerli W, Trampuz A, Oshner PE. Prosthetic-joint infections. *N Engl J Med* **2004,** 351, 1645-1654.

[2] Darouiche RO. Treatment of infections associated with surgical implants. *N Engl J Med* **2004,** 350, 1422-1429.

[3] Regi MV, Balas F, Arcos D. Mesoporous Materials for drug delivery. *Angew. Chem. Int. Ed.* **2007,** 46, 7548-7558.

[4] Langer R, Vacanti JP. Tissue engineering. *Science* **1993**, 260, 920-926.

[5] Mohamed NR, Delbert ED, B. Sonny B, Qiang F, Steven BJ, Lynda FB, Antoni PT. *Acta Biomater* **2011,** 7, 2355-2373.

[6] Ohgushi H, Caplan AI. Stem cell technology and bioceramics: from cell to the gene engineering. *J Biomed Mater Res B* **1994,** 48, 913-927.

[7] Takezawa T. A strategy for tissue engineering scaffolds that regulate cell behaviour. *Biomaterails* **2003,** 24, 2267-2275.

[8] Guarino V, Causa F, Ambrosio L. Bioactive scaffolds for bone and ligament tissue. *Expert Rev. Med. Devices* **2007,** 1, 245-260.

[9] Hutmacher DW, Schantz JT, Lam CXF, Tan KC, Lim TC. State of art and future directions of scaffolds-based bone engineering from biomaterials perspective. *J Tissue Eng. Regen. Med* **2007,** 1, 245-260.

[10] Lanza RP, Langer R, Vacanti J. Principles of Tissue Engineering. 2nd ed. Academic press, **2007.**

[11] Salgado AJ, Coutinho OP, Reis RL. Bone tissue engineering: state of art and future trends. *Macromol Biosci* **2004,** 4, 743-765.

[12] Jones JR, Ehrenfried LM, Hench LL. Optimising bioactive glass scaffolds for bone tissue engineering. *Biomaterials* **2006,** 27, 964-973.

[13] Kaur G, Pandey OP, Singh K, Homa D, ScottB, Pickrell G. A review of bioactive glasses; Their structure, properties, fabrication and apatite formation. *J Biomed Mater Res A* **2014,** 102, 254-275.

[14] Kokubo T, Takadama H. How useful is SBF in predicting in vivo bone bioactivity? *Biomaterials* **2006,** 27, 2907-2917.

[15] Kaur G, Pickrell G, Sriranganathan N, Kumar V, Homa D. Review and the state of art: Sol-gel and melt quenched bioactive glasses for tissue engineering. *J Biomed Mater Res A* **2016,** 104, 1248- 1275.

[16] Rahman MN, Day DE, Bal BS, Fu Q, Jung SB, Bonewald LF, Tomsia AP. Bioactive glass in tissue engineering. *Acta Biomater* **2011,** 7, 2355-2373.

[17] O'Donnnell MD, Watts SJ, Hill RG, Law RV. The effect of phosphate content on the bioactivity of soda-lime-phosphosilicate glasses. *J Mater Sci; Mater Med* **2009,** 20, 1611-1618.

[18] Courtheoux L, Loa J, Nedelec JM, Jallot E. Controlled bioactivity in zinc-doped sol-gel-derived binary bioactive glasses. *J Phys Chem C* **2008,** 67, 56-65.

[19] Li HC, Wang DG, Hu JH, Chen CZ. Crystallization, mechanical properties and in vitro bioactivity of sol-gel derived Na_2O-CaO-SiO_2-P_2O_5 glass-ceramics by partial substitution of CaF_2 for CaO. *J Sol-Gel Sci Technol* **2013,** 67, 56-65..

[20] de Oliveira AAR, de Souza DA, Dias LLS, de Carvalho SM, Mansur HS, de Magalha es Pereira M. Synthesis, characterization and cytocompatibility of spherical bioactive glass nanoparticles for potential hard tissue engineering applications. *Biomed Mater* **2011,** 8, 025011(14pp).

[21] Du RL, Chang J, Ni SY, Zhai WY. Characterization and in vitro Bioactivity of Zinc-containing Bioactive Glass and Glassceramics. *J Biomater Appl* **2006,** 6, 51046-51056.

[22] Garg S, Thakur S, Gupta A, Kaur G, Pandey OP. Antibacterial and anticancerous drug loading kinetics for (10-x)Cu-xZnO-20CaO-60SiO_2-10P_2O_5($2 \leq x \leq 8$) mesoporous bioactive glasses**.** *J Mater Sci: Mater Med* **2017,** 28, 1-14

[23] Kaur G, Pandey OP, Singh K, Chudasama B, Kumar V. Combined and individual doxorubic/vancomycin drug loading, release kinetics and apatite formation for Cao-CuO-P_2O_5-SiO_2-B_2O_3 mesoporous glasses. *RSC Adv* **2016,** 6, 51046-51056.

[24] Thakur S, Garg S, Kaur G, Pandey OP. Effect of Strontium substitution on the Cytocompatibility and 3-D Scaffold Structure for the xSrO-(10-x)MgO-60SiO_2-20CaO-10P_2O_5($2 \leq x \leq 8$) Sol-gel glasses. *J Mater Sci: Mater Med* **2017,** 28:89, DOI 10.1007/s10856-017-5901-z.

[25] Hutmcher DW. Scaffolds in tissue engneeering bone and cartilage. *Biomateraials* **2000,** 21, 2529-2543.

[26] Tolli H, Kujala S, LeVonen K, Jasma T, Jalovaara P. Bioglass as a carrier for reindeer bone protein extract in the healing of rat femur defect. *J Mater Sci; Mater Med* **2010,** 21, 1677-1684.

[27] Garcia A, Cicuendez M, Izquierdo- Barba I, Acros D, Vallet-Regi M. Essential role of calcium phosphate heterogeneties in 2D-hexagonal and 3D-cubic Sio2-Cao-P2O5 mesoporous bioactive glasses. *Chem Mater* **2009,** 21, 5474-5484.

[28] Wu C, Fan W, Chang J. Functional mesoporous bioactive glass nanospheres: Synthesis, high loading efficiency, controllable delivery of doxorubicin and inhibitory effect on bone cancer cells. *J Mater Chem B* **2013,** 1, 2710-2718.

[29] Hum J, Boccaccini AR. Bioactive glasses as carriers for bioactive molecules and therapeutic drugs: A review. *J Mater Sci; Mater Med* **2012,** 23, 2317-2333.

[30] Allen TM, Cullis PR. Drug delivery systems: Entering the main stram. *Science* **2004,** 303, 1818-1822.

[31] Li L, Clark AE, Hench LL. An investigation of bioactive glass powders by sol-gel processing. *J Appl Biomater* **1991,** 2, 231-239.

[32] Regi MV, Izquierdo- Barba I, Calilla M. Review: Structure and functionalization of mesoporous bioceramics for bone tissue regeneration and local drug delivery. *Phil Trans R Soc Lond A* **2001,** 370, 1400-1421.

[33] Zhu M, Zhang L, He Q, Zhao J, Limin G, Shi J. Mesoporous bioactive glass-coated poly(L-lactic acid) scaffolds: a sustained antibiotic drug release system for bone repairing. *J Mater Chem B* **2001,** 21, 1064-1072.

[34] MourinoV, Baccaccini AR. Bone tissue engineering therapeutics: Controlled drug delivery in three-dimensional scaffolds. *J R Soc Interface* **2009,** 7, 209-227.

[35] Regi MV, Ramila A, del Real RP, Perez-Parienete J. A new property of MCM-41: drug delivery system. *Chem Mater* **2001,** 13, 308-311.

[36] Yan X, Yu C, Zhou X, Tang J, Zhao D. Highly ordered mesoporous bioactive glasses with superior in-vitro bone-forming boactivities. *Angew Chem Int Ed Engl* **2004,** 43, 5980-5984.

[37] Wu C, Chang J. Mesoporous bioactive glasses: structure characteristics, drug/growth factor delivery and regeneration application. *Interface Focus* **2012,** 2, 292-306.
[38] Regi MV. Ceramics for medical applications. *Dalton Trans* **2001,** 2, 97-108.
[39] Iler RK. The chemistry of silica. New York: Wiley, **1995.**
[40] Frickle J, Caps R. In: Ultrastructure processing of Advanced Ceramics. Mackenzie JD, Ulrich DR, editors. New York: Wiley, **1988.**
[41] Brinker CJ, Scherer GW, Roth EP. Sol-Gel-glass: Physical and structural evolution during constant heating rate experiments. *J Non-Cryst Solids* **1985,** 72, 345-368.
[42] Coltrain BK, Melpolder SM, Salva JM. Infrastructure Processing of Advanced Materials . Uhlmann DR, Ulrich DR, editors. Wiley: New York; **1992.**
[43] Xia W, Chang J. Well-ordered mesoporous bioactive glasses (MBG): A promising bioactive drug delivery system. *J Control Release* **2006,** 110,522-530.
[44] Hoffmann F, Cornelius M, Morell J, Froba M. Silica-based mesoporous organic-inorganic hybrid materials. *Angew Chem* **2003,** 118, 3290-3328.
[45] Mal K, Fujiwara M, Tanaka Y. Photocontrolled reversible release of guest molecules from coumarin-modified mesoporous silica. *Nature* **2003,** 421, 350-352.
[46] Bigucci F, Luppi B, Cerahiarac T, Sorrenti M, Bettinetti G, Rodriguez L, Zecchi V. Chitosan/pectin polyelectrolyte complexes; Selection of suitable preparative conditions for colon-specific delivery of vancomycin. *Eur. J. Pharm. Sci.* **2008,** 35, 435-441.
[47] Xie Z, Lui X, Jia W, Zhang C, Huang W, Wang J. Treatment ostcomuelitis and repair of bone defect by degradable bioactive borate glass releasing vancomycin. *J Control Release* **2009,** 139, 118-126.
[48] Nagaranjan R,. Glycopeptide Antibiotics. Indian: Lilly Research Laboratories ElinLlilly and Company Indianapolis **1994.**
[49] Tacara O, Sriarnornsakb P, Dassa CR. Doxorubicin: am update on anticancer molecular action, toxicity and novel drug delivry systems. *J Pharm Pharmacol* **2013,** 65, 157-170.
[50] Allwood M, Stanley A, Wright P. The cytotoxics Handbook, 4th ed; **2002.**
[51] Rainsford KD. Ibuprofen: A critical bibliographic review. Sheffield, UK: Sheffield Hallan University **2003.**
[52] Balas F, Manzano M, Horcajada P, Regi MV. Confinement and controlled release of bisphosphonates on ordered mesoporous silica-based materials. *J Am Chem Soc* **2006,** 128, 8116-8117.
[53] Doadrio AL, Sousa EMB, Doadrio JC, Pariente JP, Izquierdo BI. Mesoporous SBA-15 HPLC evaluation for controlled gentamicin drug delivery. *J of Control Release* **2004,** 97, 125-132.
[54] Barba II, Martinez A, Doadrio AL, Pariente JP, Regi MV. Release evaluation of drugs from orderd three-dimensional silica structures. *Eur J Pharm Sci* **2005,** 26, 365-373.
[55] Zeng W, Qian XF, Zhang YB, Yin J, Zhu ZK. Organic modified mesoporous MCM-41 through solvothermal process as drug delivery system. *Eur J Pharm Sci* **2005,** 26, 365-373.
[56] Kokubo T. bioactive glass ceramics: Properties and applicationa. *Biomaterials* **1991,** 12, 155-163.
[57] Lee K.Y.; Peters, M. C.; Mooney, D. J. *Adv. Mater.,* **2001,** 13, 837-839.
[58] Lasic, D. D. *Polymer news,* **1998,** 23, 367-375.
[59] Brannon-peppas, L.; Birnbaum, D.T.; Kosmala, J.D. *Polymer news,* **1997,** 22, 316-318.
[60] Uhrich, K. E.; Cannizaaro, S. M.; Langer, R.S. *Chem. Rev.,* **1999,** 99, 3118-3198.
[61] Langer, R. S. *Nature,* **1998,** 392-395

CHAPTER- 2

LITERATURE REVIEW

2.1. General

Biomaterials development especially bioactive glasses has become a promising research field for applications in bone tissue engineering. The aim of tissue engineering is to restore diseased or damaged tissue to its natural state and restore their functioning using combination of stem cells and scaffolds [1-2]. The first generation of materials used for replacement of tissue are known as bio-inert materials and they have resulted in loosening and breakdown of tissue with time. Therefore, bioactive materials were discovered for the tissue replacement with the capability of forming bond with the living tissues [3]. The versatile properties of bioactive glasses such as non-mutagenic, non-carcinogenic and non-antigenic make them suitable for the tissue engineering [4]. The first bioglass 45S5 was invented by Hench, consists of 45% SiO_2, 24.5% CaO, 24.5% Na_2O and 6% P_2O_5 by weight percent [5].

Considering research carried out in the last 15 years, this chapter contains literature review about the work of researchers in the development and application of bioactive glasses as drug loading carriers and controlled-release systems. The first drug delivery vehicle used in 2001 was MCM-41. Large surface areas and well ordered pore network make mesoporous materials suitable candidates for drug delivery. Moreover, highly ordered mesoporous channels helps in loading and releasing large amount of drugs [6-7]. This chapter also presents the work performed by various researchers about the preparation of simulated biological fluids having ion concentrations equal to or close to human blood plasma for assessment of bioactivities of different materials [8]. Bioactive glasses are soaked in simulated body fluids, which results in the formation of hydroxyapatite (HA) layer on their surface which is responsible for forming a bond with the living tissue [9]. Melt quenching and sol-gel are the most common techniques for the fabrication of bioactive glasses [10, 11-13]. The silica content in sol-gel derived glasses should be upto 90 mol% silica so as to allow HA layer formation and bone bonding [14].

Li *et al.* [15] had fabricated gentamicin-loaded mesoporous bioactive glass (MBG) for use as antibiotic in controlled drug delivery system. Gent-MBG exhibited sustained release of gentamicin in the local sites of bone defects for more than 6 days so as to prevent orthopedic

peri-implant infections. Gent-MBG has reduced the bacterial adhesion of biofilm formation of S.aureus (ATCC25923) and S.epidermides (ATCC35984). MBG had an advantage of high drug loading efficiency (79-83%) than non- mesoporous bioactive glass (NBG) (18-19%). Biocompatibility of MBG can be tested with human bone marrow stromal cells (hBMSCs). It was found that MBG had excellent biocompatibility than NBG due to its mesoporous structure and high surface area. Large surface areas of MBG allow a large amount of Si-O bonds to interact with gentamicin molecules through amino and hydroxl groups. Pore size of approximately 3 nm and large pore volume (0.900 cm^3/g) creates sufficient space for gentamicin to reach the inside of MBGs.

Arcos *et al.* [16] worked with loading of gentamicin sulfate in composites made from a SiO_2-CaO-P_2O_5 bioactive glass and polymethylmethacrylate composite. The bioactive behavior of the glass makes it a desirable material in the drug delivery system. When the glass was soaked in the simulated body fluid (SBF), then release kinetics indicate that composites supply high doses of antibiotics. 'Maintenance' doses were supplied by a slower drug release rate till the end of the experiment. The release rate of gentamicin depends on the Ca^{2+} and H_3O^+ ionic exchange between composite and SBF. Porous structure of composites was responsible for the formation of hydroxycarbonate apatite on the surface and into the pores.

Arcos *et al.* [17] prepared bioactive microspheres belonging to SiO_2-CaO-P_2O_5 systems by an EISA process. The structure directing agent and its interaction with Ca^{2+} was used for determining the mesoporous structure. For any CaO content, cetyltrimethyl ammonium bromide (CTAB ionic surfactant) does not produce mesopores at the external surface while P123 (nonionic triblock copolymer) can produce wormlike mesoporous structures. For low CaO content, F127 (triblock copolymer) leads to hexagonal ordered structures. When reacted with SBF, an apatite like layer was formed by all the mesoporous SiO_2-CaO-P_2O_5 mesopores. Bioactive behavior and drug release properties of these materials proved their ability to act as a drug delivery system.

Wu *et al.* [18] successfully prepared bioactive MBG nanospheres with combined dual functions of drug delivery and bioactivity by using a facile hydrothermal method. Anticancer drug DOX, incorporated in the MBG nanospheres showed high drug loading efficiency of around 90%. By adjusting the initial drug loading concentration and pH microenvironment, the loading and

release kinetics of DOX can be efficiently controlled. The viability of bone cancer cells was inhibited by DOX released by MBG nanospheres. The unique characteristics of MBG nanospheres such as excellent apatite-mineralization ability, distinct degradation rate and controllable release of anticancer drug make it a promising drug carrier for bone cancer therapy.

Wu *et al.* [19] summarized recent research advances of MBG in the past several years. The effect of mesopore templates and composition on the mesopore-structure characteristics, MBG as a drug carrier and the functional effect on the anti-bacteria and tissue-stimulation properties are also highlighted. Mesoporous structure of MBG particles could improve their loading efficiency i.e. they could load drugs with 50% loading efficiency. Generally, as compared to P123- and F127- induced MBGs, CTAB- induced MBGs have better drug delivery properties.

Wu *et al.* [20] fabricated a bioactive $SrO\text{-}SiO_2$ glass by the incorporation of Sr^{2+} into SiO_2. As compared to mesoporous SiO2, mesoporous Sr-Si glass has an improved mesopore structure (mesopore size, pore volume and specific surface area) as well as dissolution and protein adsorbtion at about 10% Sr content. By altering the Sr content in mesoporous Sr-Si glass particles, the release profile of bioactive Sr^{2+} ions and a model drug DEX can be controlled. Porous scaffolds prepared from mesoporous Sr-Si glasses show a more sustained drug release.

Kaur *et al.* [21] used sol-gel technique for the preparation of MBG series $(25\text{-}x)CaO\text{-}xCuO\text{-}10P_2O_5\text{-}5B_2O_3\text{-}60SiO_2$ (x=2.5, 5, 7.5, 10). The surface area of MBG varies from 281-418 m^2/g, while pore size lies between 6.1-9.1 nm. Antibacterial and anticancerous drugs vancomycin (VANCO) and DOX were loaded in MBGs. To investigate the effect of combined loading on the release capability of MBGs, both the drugs were loaded together. The increasing copper content influenced the drug loading and release kinetics of the DOX and VANCO as well as the bioactive properties.

Garg *et al.* [22] studied drug loading kinetics of antibacterial drugs vancomycin (VANCO) and tetracycline (TETRA) as well as anticancerous drug DOX for the MBGs of composition $(10\text{-}x)CuO\text{-}xZnO\text{-}20CaO\text{-}60SiO_2\text{-}10P_2O_5$ (x=2, 4, 6, 8). Immersion in SBF for 15 days revealed HA layer formation on the surface of MBGs. The specific surface area of MBGs varied from 263-402 cm^2/g while the range of pore size lies between 4.2-9.7 nm. The drugs were loaded in MBGs

among, which VANCO was almost fully loaded while the decreasing copper content shows variation in loading properties of other drugs DOX and TETRA.

Thakur *et al.* [23] synthesized xSrO-(10-x)MgO-60SiO_2-20CaO-10P_2O_5 (x=2, 4, 6,8) sol-gel glasses and evaluate their mechanical, physical and biocompatible properties. The cytotoxicity assays were conducted for MG63 human osteosarcoma cell line. By using polymer replication method, the as-prepared glasses were used for the fabrication of 3-D porous scaffolds. The glasses were sintered at different temperatures i.e. 700º C, 800º C, 900º C for about 6 hr so as to densify the glass network and the effect of the sintering temperature on the properties and structure of as prepared scaffolds were also analyzed.

Soundrapandian *et al.* [24] developed two new glasses with compositions based on SiO_2-Na_2O-ZnO-CaO-MgO-P_2O_5 system (hereafter referred to as BGZ and MBG). A porous scaffold made of these bioactive glasses has been reported to act as drug delivery system for the treatment of bone infections. Using vaccum infiltration method, gatifloxacin (GAT) drug was loaded into the porous scaffold. Orthopedic infections can be treated by successful drug releasing of 63-66% porous and 5-50 µm unimodal porous MBG and BGZ bioactive glass scaffolds in 43 days. Fickian diffusion based Peppas-Korsmeyer release pattern was followed by release of drug, while burst release and overall release of drug was decreased by 0.5-1% chitosan coating on scaffolds. BGZ was found to be mildly cytotoxic with moderate wound healing potential while biocompatibility, bioactivity, non-cytotoxicity and excellent wound healing potential were exhibited by the MBG based scaffolds.

Gao *et al*. [25] modified biomodal mesoporous silica with 3-aminopropyltriethoxysilane so as to use it as carrier for aspirin loading and release. MCM-41, the unimodal mesoporous material was also modified as the aspirin carrier for exploring the effects on drug delivery behavior. For unrestricted drug molecules diffusing, biomodal mesopores are found to be beneficial and helps in loading and releasing large amount of drugs. The existence of the large pore of biomodal mesoporous silica has great influence on drug delivery properties.

Zhang *et al*. [26] used the method of alginate cross-linking with Ca^{2+} for the preparation of Samarium (Sm) incorporated MBG microspheres. Immersion in SBF indicates the in vitro bioactivities of microspheres and faster apatite formation rate on the surface. DOX drug was

loaded in the microspheres for the investigation of drug delivery properties and are found to exhibit sustained DOX delivery. By changing the values of pH microenvironment and doping concentration of Sm, drug delivery from Sm/MBG/alginate microspheres can be dominated.

Zhang *et al*. [27] fabricated both mesoporous silica (MS) and MBG through an evaporation induced self-assembly method (EISA). Ibuprofen (IBP) drug was encapsulated in both the samples. The investigation results indicated that the stronger interaction between IBP and Ca^{2+} of MBG, high surface area and pore volume helps in high drug loading efficiency (46%) of MBG than that of MS (28%). It was found that MBG had a long drug release process as compared to MS. The drug release process was also affected by the biodegradation and hydroxyapatite (HA) growth of the host materials. High drug loading efficiency and controlled release effect of MBG make it a suitable candidate for the drug delivery.

Lin *et al*. [28] synthesized folate (FA)-modified MBG and used it as anticancer drug for the investigation of receptor-mediated targeting characteristics. A water insoluble anticancer drug camptothecin (CPT) was delivered into the cancer cells. Increased cell uptake of anticancer drug delivery vehicles mediated by the FA receptor helps the CPT-loaded MBG-FA to exhibit greater cytotoxicity than free CPT.

Wang *et al*. [29] synthesized MBG scaffolds consisting of micropores using P123 as mesopore soft template and Mediterranean sea sponge as macropored hard template. MBG wall was used for maintaining the structure and morphology of the Mediterranean sea sponges. Dexamethasone (DEX) was incorporated as a drug. The drug release profiles showed the sustained drug delivery capability of the dual porous materials. Due to excellent apatite mineralization ability of well ordered dual pore MBG materials, they can be used as a bioactive drug release system.

Baino *et al*. [30] prepared MBG membranes (SiO2-P2O5-CaO) using sol-gel method coupled with an EISA process. A non-ionic block co-polymer was used as a mesostructure former. IBP drug was loaded into MBG pores and MBG membranes were soaked in SBF for the investigation of drug release kinetics. The results showed that prepared MBG (5 nm) and mesoporous silica have similar drug release kinetics in SBF. The prepared materials can be use as "smart" multifunctional grafts for bone reconstructive surgery because of several features such as high

bioactivity and biocompatibility, drug-loading efficiency and higher ability to induce HA layer formation on its surface.

Hum *et al.* [31] presented different compositions and morphologies of various bioactive glasses used as a drug/biomolecule carrier. To combine the attractive properties of the glass with the specific therapeutic effect of the drug/biomolecule, BGs are being considered as the carriers for therapeutic drugs and bioactive molecules in the field of bone regeneration. Incorporation of therapeutic drug/bioactive molecule during the manufacturing of sol-gel derived BGs have an advantage of direct interaction of molecules with the phosphate and hydroxl groups of the glass and hence is the most efficient loading procedure. Soaking BG samples in solutions with the desired molecules is least efficient method of drug loading. During the first hours of immersion, these carriers release 80-90% of the loaded molecules into different aqueous media.

Xue *et al.* [32] synthesized a poly (D, L-lactide-co-glycolide) (PLGA)/mesopoous silica hybrid structure (PS hybrid structure) using novel sol-gel route followed by single emulsion solvent evaporation. Drug release behaviors of PS hybrid structure and mesoporous silica (MS) were studied. It was found that during the first day GENT-loaded MS without any encapsulation showed a sharp initial burst followed by slow release of drugs over a period of 3 weeks. Drug release period of hybrid structure could last as long as 5 weeks. Hybrid microspheres show three different behaviors during the drug release i.e. an initial burst, a plateau stage with a slow release rate, followed by a constant release stage. The initial release burst (27.4 wt%) of the hybrid structure was reduced significantly thus making it a promising drug release material for bone filling applications.

Gao *et al.* [33] manufactured hollow mesoporous silica nanoparticles (HMSNs) with three different pore sizes so as to control the drug release rate. Multidrug-resistant (MDR) cancer cells were used to evaluate the biological roles of these HMSNs. Toward drug-sensitive MCF-7 and drug-resistant MCF-7/ADR cells, HMSNs showed negligible cytotoxicity. DOX incorporated HMSNs could mediate efficient cellular uptake of DOX and more intracellular drug accumulation. Pore-size dependent anticancer activity against MCF-7/ADR cells was also exhibited by DMSNs.

Prokopowicz *et al.* [34] synthesized and evaluated precursors of calcium and phosphorous as implantable bioactive drug delivery systems. An anticancer drug DOX was encapsulated in a sol-gel derived silica and silica-plydimethylsiloxane (silica-PDMS) composites. The results showed that by controlling two independent factors: the addition of polydimethylsiloxane and the amount of calcium chloride, the release rate of DOX can be effectively controlled. It was also found that increasing amount of calcium precursor increased the delivery rate of DOX. In silica-PDMS system, constant rate of DOX release was observed.

Radin *et al.* [35] worked on controlled release silica sol-gels. Sol-gels released a lot of molecules including proteins, growth factors and drugs and the quantity and duration of drug release can vary widely. A two step process was used to synthesize these sol gel microspheres: acid-base catalyzed hydrolysis followed by emulsification. The drugs, which were incorporated in microspheres, showed a slower, long –term release in contrast to rapid, short-term release from ground granules. Sol-gel granules prepared by grinding and sieving had different in vitro release properties from the sol gel microspheres.

Martin *et al.* [36] worked on transdermal drug delivery applications with sugar glass microneedles (MNs). The barrier properties of outer skin layer limit transdermal drug delivery. Combination solution of sucrose sugar and dehydration of trehalose created the solid amorphous sugar glasses containing low residual quantities of water. Even though biodegradable MNs offer various advantages, but processing commonly requires elevated temperatures, that can adversely affect heat-labile molecules and macromolecules. Sugar glass MNs dissolved rapidly and completely in situ releasing dye into deeper skin layers by incorporating a marker compound.

Massaro *et al.* [37] fabricated covalently functionalized halloysite nanotubes (HNTs), which are successfully employed as dual-responsive nanocarriers for curcumin (Cur). HNT-Cur prodrug was synthesized with controlled Cur release depending on glutathione (GSH) and pH condition. Through disulphide linkage, halloysite is firstly functionalized with cysteamine to obtain HNT-Cur prodrug. Afterwards, via Schiff's base formation, Cur molecules are chemically conjugated to amino end groups of halloysite. Thermogravimetric analysis, dynamic light scattering, FT-IR spectroscopy and scanning electron microscopy (SEM) proved successful functionalization of halloysite. On HNT external surface, presence of Cur was confirmed with experimental data.

Bigi *et al.* [38] tested in vitro bioactivity of gelatin sponges and HA-enriched gelatin sponges after soaking in 1.5 SBF for 21 days at 37ºC. The presence of HA crystals inside HA-gelatin sponges act as catalysts for the deposition of bonelike apatite crystals. The mean diameter of spherical aggregates increased from about 1-2 μm, after 4 days of soaking in SBF solution, up to about 3.5 μm in the samples soaked for 21 days. The relative amount of inorganic phase (poor crystalline carbonated apatite) laid down on HA-gelatin sponges increased upto 56 wt% leading to a composite material with composition similar to that of trabecular bone apatite.

Muller *et al.* [39] prepared SBF with different HCO_3^- content and tested the bioactivity of bone and dental implant materials. Common SBF has a higher Cl^- and a lower HCO_3^- concentration. By using HCO_3^- concentrations ranging from 5 to 27 mmol/l five different SBFs with a composition of 142 Na^+, 5K^+, 2.5 Ca^{2+}, 1 Mg^{2+}, 1 SO_4^{2-}, 1 HPO_4^{2-} and 136 (Cl^- + HCO_3^-) mmol/l were prepared. High stability of prepared SBF enables the assessment of HA formation on the surface of bioactive materials. The SBF solutions were shown to be supersaturated as compared to carbonated apatite. HCO_3^- content in SBF influences the composition as well as the structure of the calcium phosphates obtained.

Lukito *et al.* [40] used various amount ratios of bioactive glass to SBF (10, 5, 3.3, 2.5 and 2 mg/ml) for testing the bioactivity of 70 wt% SiO_2-30 wt% CaO bioactive glass. During the first 6 h, HA crystalline phase was formed on the surfaces of all the BGs, due to the high concentration of PO_4^{3-} in the original SBF solutions. The four SBF solutions (10, 5, 3.3 and 2.5) were supersaturated for calcite after 6 h of soaking. There is no calcite crystalline phase formed on the surface of the BGs with the amount ratio of 2 mg/ml.

Puga *et al.* [41] suggested that prevention and treatment of osteomyelitis could be achieved through local drug delivery using implantable devices, which provide therapeutic levels at the infection side with minimum side-effects. Physical blends of polycaprolactone (PCL) and poloxamine (Tetronic) were prepared by applying a solvent-free hot melting approach to obtain cytocompatible implants with a tunable bioerosion rate, ciprofloxacin release profile and osteoconductive features. Incorporation of the block copolymer at weight ratio ranging from 25 to 75 wt% led to matrices with viscoelastic parameters. Once immersed in buffer, the matrices underwent a similar weight loss in the first week to the content of poloxamine, followed by a slower erosion rate due to PCL.

Since, lots of work has been done by many research groups in the applications of BGs as carriers for drug delivery. The work of our group has been focused on developing novel MBG using sol-gel technique and CTAB as structure directing agent for the drug delivery of anticancerous and antibacterial drugs. Our group has already synthesized mesoporous glass series of composition $CaO–CuO–P_2O_5–B_2O_3–SiO_2$ [21], $CuO\text{-}ZnO\text{-}CaO\text{-}SiO_2\text{-}P_2O_5$ [22], $SiO_2\text{-}BaO\text{-}ZnO\text{-}B_2O_3\text{-}Al_2O_3$ [10] and $SrO - MgO - SiO_2 – CaO - P_2O_5$ [23]. In the present study, our group synthesized glass-ceramic of composition $CuO\text{-}MgO\text{-}P_2O_5\text{-}SiO_2\text{-}CaO\text{-}ZnO$ and it is highly bioactive in nature. The effect of BG content and the percentage of drug loaded and released are investigated. The novelty of this work is that, no report has been described in literature using the given composition. It is studied that BGs can stimulate bone growth and can bond to both bone and soft tissue. They have the ability to form a surface layer of HCA [42-43]..

REFERENCES

[1] Hench LL, Polak JM. Third-generation biomedical materials. *Science* **2002,** 295, 1014-1017.

[2] Williams D. Benefit and risk in tissue engineering. *Mater. Today* **2004,** 7, 24-29.

[3] Hench LL, Day DE, Holand W, Rheinberger VM. *IJAGS* **2010**, 1, 104-117.

[4] Kaur G, Pickrell G, Sriranganathan N, Kumar V, Homa D. Review and the state of art: Sol-gel and melt quenched bioactive glasses for tissue engineering. *J Biomed Mater Res A* **2016,** 104, 1248- 1275.

[5] Hench LL. The story of bioglass VR. *J Mater Sci: Mater Med* **2006,** 17, 967-968.

[6] Wu C, Zhou Y, Lin C, Chng J, Xiao Y. Strontium- containing mesoporous bioactive glass scaffolds with improved osteogenic/cementogenic differentiation of periodontal ligament cells for periodontal tissue engineering. *Acta Biomater***2012,** 8, 3805-3815.

[7] Cicuendez M, portoles MT, Izquierdo-Barba I, Vallet-Regi M. New nanocomposite system with nanocrystalline apatite embedded into mesoporous bioactive glass. *Chem Mater***2012,** 8, 3805-3815.

[8] Oyane A, Kim HM, Furuya T, Kokubo T, Miyazaki T, Nakamura T. *J Biomed Mater Res A* **2003,** 65, 188-195.

[9] Clark AE, Hench LL. The influence of surface chemistry on implant interface. *J Biomed Mater Res* **1976,** 10, 161- 174.

[10] Kaur G, Sharma P, Kumar V, Singh K. Assessment of in-vitro bioactivity of SiO_2-BaO-B_2O_3-Al_2O_3 glasses. An optico-analytical approach. *Mater Sci Eng C* **2012**, 32, 1941-1947.

[11] Madanat R, Moritz N, Vedel E, Svedsto E, Aro HT. Radio-opaque bioactive glass markers for radiostereometric analysis. *Acta Biomater* **2009,** 5, 3497-3505.

[12] Kingery WD, Bowen HK, UhlmannDR. introduction to Ceramics, 2nd ed. New York: Johan Wiley and Sons; **1976.**

[13] Shelby JE. Introduction to glass science and technology, 2nd ed. Cambridge: The Royal Society of Chemistry; **2005.**

[14] Sepulveda P, Jones JR, Hench LL. Bioactive sol-gel foams for tissue repair. *J Biomed Res A* **2002**, 49, 340-348.

[15] Li Y, Liu YZ, Long T, YuXB, Tang TT, Dia KR, Tian B, Guo YP, Zhu ZA. Mesoporous bioactive glass as drug delivery: fabrication, bactericidal properties and biocompatibility. *J Mater Sci; Mater Med* **2013,** 24, 1951-1961.

[16] Arcos D, Ragel CV, Vallet-Regi M. Bioactivity in glass/PMMA composite used as drug delivery system, *Biomaterials* **2001,** 22, 701-708.

[17] Arcos D, Lopez-Noriega A, Ruiz-Hernandez E, Terasaki O, Vallet-Regi M. Ordered Mesoporous Microspheres for bone Grafting and Drug Delivery. *Chem Mater* **2009,** 21, 1000-1009.

[18] Wu C, Fan W, Chang J. Functional mesoporous bioactive glass nanospheres: Synthesis, high loading efficiency, controllable delivery of doxorubicin and inhibitory effect on bone cancer cells. *J Mater Chem B* **2013,** 1, 2710-2718.

[19] Wu C, Chang J. Mesoporous bioactive glasses: structure characteristics, drug/growth factor delivery and regeneration application. *Interface Focus* **2012,** 2, 292-306.

[20] Wu C, Fan W, Gelinsky M, Xiao Y, Simon P, Doert T, Luo Y, Cuniberti G. Bioactive Sro-Sio_2 glass with well-ordered mesopores: characterization, physiochemistry and biological properties. *Acta biomater* **2011**, 7, 1797-1806.

[21] Kaur G, Pandey OP, Singh K, Chudasama B, Kumar V. Combined and individual doxorubic/vancomycin drug loading, release kinetics and apatite formation for CaO-CuO-P_2O_5-SiO_2-B_2O_3 mesoporous glasses. *RSC Adv* **2016,** 6, 51046-51056.

[22] Garg S, Thakur S, Gupta A, Kaur G, Pandey OP. Antibacterial and anticancerous drug loading kinetics for (10-x)Cu-xZnO-20CaO-60SiO_2-10P_2O_5($2\leq x\leq 8$) mesoporous bioactive glasses**.** *J Mater Sci: Mater Med* **2017,** 28, 1-14.

[23] Thakur S, Garg S, Kaur G, Pandey OP. Effect of Strontium substitution on the Cytocompatibility and 3-D Scaffold Structure for the xSrO-(10-x)MgO-60SiO_2-20CaO-10P_2O_5($2\leq x\leq 8$) Sol-gel glasses. *J Mater Sci: Mater Med* **2017,** 28:89, DOI 10.1007/s10856-017-5901-z.

[24] Soundrapandian C, Mahato A, Kundu B, Datta S, Sa B, Basu D. Development and effect of different bioactive silicate glass scaffolds: In vitro evaluation for use as a bone drud delivery system. *J Mech Behav Biomed Mater* **2014**, 40, 1-12.

[25] Gao L, Sun J, Li Y. Functinalized bimodal mesoporous silicas as carriers for controlled aspirin delivery. *J Solid State Chem* **2011,** 1184, 1909-1914.

[26] Zhang Y, Wang X, Su Y, Chen D, Zhong W. A doxorubicin delivery system: Samarium/mesoporous bioactive glass/alginate composite microspheres. *Mater Sci Eng C* **2016,** 67, 205-213.

[27] Zhang J, Qu FY, Lin HM, Wu X, Jiang JJ. Mesoporous bioactive glass: ideal material for higher uptake and well sustained release of Ibuprofen. *Mater Res Innov* **2012,** 16, 230-235.

[28] Lin HM, Lin HY, Chan MH. Preparation, characterization and in vitro evaluation of folate-modified mesoporous bioactive glass for targeted anticancer drug carriers. *J Mater Chem B* **2013**, 1, 6147--6156.

[29] Wang H, Gao X, Wang Y, Tang J, Sun C, Deng X, Niu X. Bio-templated synthesis of mesoporous bioactive glass with a hierarchical pore structur. *Mater Lett* **2012,** 76, 237-239.

[30] Baino F, Fiorilli S, Mortera R, Onida B, Saino E, Visai L, Verne E, Vitale-Brovarone. Mesoporous bioactive glass as a multifunctional system for bone regeneration and controlled drug release. *J Appl Biomater Func Mater* **2012**, 10, 12-21.

[31] Hum J, Boccaccini AR. Bioactive glasses as carriers for bioactive molecules and therapeutic drugs: A review. *J Mater Sci; Mater Med* **2012,** 23, 2317-2333.

[32] Xue JM, Shi M. PLGA/mesoporous silica hybrid structure for controlled drug release. *J Control Release* **2004,** 98, 209-217.

[33] Gao Y, Chen Y, Ji X, He X, Yin Q, Zhang Z, Shi J, Li Y. Controlled Intracellular release of Dexorubicin in Multidrug-Resistant Cancer Cells by Tuning the Shell-Pore Sizes of Mesoporous Silica Nanoparticles. *ACS Nano* **2011**, 5, 9788-9798.

[34] Prokopowicz M, Nski JZ, Gandhi A, Sawicki W, Tofail SAM. Bioactive silica-based drug delivery systems containing doxorubicin hydrochloride: In vitro studies. *Colloids and Surfaces B: Biointerfaces* **2012**, 93, 249-259.

[35] Radin S, Chen T, Ducheyne P. The controlled release of drugs from emulsified, sol-gel processed silica microsphers. *Biomater* **2009**, 30, 850-858.

[36] Martin CJ, Allender CJ, Brain KR, Morrissey A, Birchall JC. Low temperature fabrication of biodegradable sugar glass microneedles for transdermal drug delivery applications. *J Control Release* **2012**, 158, 93-101.

[37] Massaro M, Amorati R, Cavallaro G, Guernelli S, Lazzara G, Milioto S, Noto R, Poma P, Riela S. Direct chemical grafted curcumin on halloysite nanotubes as dual-responsive prodrug P, for pharmacological applications. *Colloids Surf B Biointerfaces* **2016,** 140,505-513.

[38] Bigi A, Boanini E, Panzavolta S, roveri N, Rubini K. Bonelike apatite growth on hydroxypatite-gelatin sponges from simulated body fluid. *J Biomed Mater Res* **2002**, 4, 709-715.

[39] Muller L, Muller LB. Preparation of SBF with different HCO#-content and its influence on the composition of biomimetic apatites. *Acta Biomater* **2006**, 2, 181-189.

[40] Lukito D, Xue JM, Wang J. In vitro bioactivity assesment of 70(wt%) SiO_2 - 30(wt%) CaO bioactive glasses in simulated body fluid. *Mater Lett* **2005**, 59, 3267-3271.

[41] Puga AM, Rey-Rico A, Magarinos B, Alvarez-Lorenzo C, Concherio A. hot melt poly-caprolactone/poloxamine implantable matrices for sustained delivery of ciprofloxacin. *Acta Biomater* **2012**, 8, 1507-1517.

[42] Kaur G. Bioactive glasses: potential biomaterials for future therapy. Germany, Heidelberg: Springer, **2017**.

[43] Kaur G. Clinical Applications of Biomaterials: State-of-the-Art Progress, Trends, and Novel Approches. New York, USA: Springer, **2017**.

CHAPTER-3
EXPERIMENTAL DETAILS

3.1.General

This chapter includes the materials and methodology and various characterization techniques used during the present investigation. Glasses were prepared using sol-gel technique and were further investigated for drug loading. The as prepared samples were characterized using various techniques such as XRD, UV visible spectroscopy, BET, and cytotoxicity test using human osteosarcoma cell line MG63.

3.2. Raw materials used

Purely organic raw materials with purity content was ≥ 99% were used. In the present study, cetyltrimethylammoniumbromide (CTAB Sigma-Aldrich) was used as a catalyst for hydrolysis. Other constituents that were used for preparing the samples were tetraethylorthosilane TEOS (≥99% purity Sigma-Aldrich), triethyl phosphate TEP (≥98% purity Sigma-Aldrich), calcium nitrate tetrahydrate $Ca(NO_3)_2.4H_2O$ (extra pure Sigma-Aldrich), zinc nitrate hexahydrate $Zn(NO_3)_2.6H_2O$ (≥99% purity Sigma-Aldrich), cupric nitrate trihydrate $Cu(NO_3)_2.3H_2O$ (extra pure Sigma-Aldrich) and magnesium nitrate hexahydrate $Mg(NO_3)_2.6H_2O$ (≥99% purity Sigma-Aldrich). All the materials mentioned above were used without any further purification.

3.3. Fabrication of mesoporous glass samples

Copper and Magnesium based bioactive glasses with chemical composition (15-x)CuO-xMgO-$10P_2O_5$-$60SiO_2$-10CaO-5ZnO ($2.5 \leq x \leq 12.5$) were prepared by mixing raw materials in the organic form of cetyltrimethylammoniumbromide (CTAB), CaO, ZnO, SiO_2, P_2O_5, MgO and CuO by sol-gel technique. These samples were prepared using appropriate mole fraction of these chemicals. Mole fraction of these chemicals is listed below in table 3.1.

Table 3.1 : Glass compositions (mol %) with their labels.

Sample label	CuO	MgO	P_2O_5	SiO_2	CaO	ZnO
GMg2.5	12.5	2.5	10	60	10	5
GMg5	10	5	10	60	10	5
GMg7.5	7.5	7.5	10	60	10	5
GMg10	5	10	10	60	10	5
GMg12.5	2.5	12.5	10	60	10	5

3.3.1. Methodology

In sol-gel technique, organic precursors were used whose purity content must be ≥ 99%. In present work, all the raw materials (precursors) were mixed in specific mole fractions listed in above table 3.1. While stirring violently, in 25 ml of ethanol, 1.5 g of CTAB is dissolved. For preparing GMg2.5 sample, 4.8 ml of triethyl phosphate (TEP) was added to 18.7 ml of tetraethylorthosilicate (TEOS) with continuous stirring. The hydrolysis of TEOS + TEP solution was catalyzed by using 1 M HNO_3, by keeping the molar ratio to be HNO_3 + deionized water: TEOS + TEP = 8:1. To promote hydrolysis mechanism the solution was stirred for 2 h. Then 0.9 g magnesium nitrate hexahydrate, 3.3 g calcium nitrate tetrahydrate, 2.08 g zinc nitrate hexahydrate and 4.34 g cupric nitrate trihydrate were added after each other at an interval of 30 min with violent stirring and the mixture was stirred well for another 2 h. The prepared sol was then kept to undergo gelation. Following this, the dried gel was kept in oven at 100°C for about 6 days for complete drying.

3.4. Characterizations of samples

As prepared samples were then characterized using various techniques to know the initial and transformed structure along with material, bioactive and drug loading properties of samples. The details of these characterization techniques are given below:

3.4.1. X-ray diffraction (XRD)

XRD is a non-destructive, rapid analytical technique used for phase identification of a crystalline material. PANalytical Xperts pro. MPD diffractometer with CuK_α radiations (λ = 1.5415 Å) was used to record X-ray powder diffraction pattern at room temperature. For most of the samples the

XRD pattern are generally taken in the range of $10^o \leq 2\theta \leq 70^o$ at a scanning speed of 2^o /min. The analyzed material is finely ground and homogenized so that all crystallographic directions are sampled by beam. The interplaner spacing of the unknown samples using Bragg's law are determined by using X-rays. The glass powder was heat treated at 700 ^{o}C for 24 h. The standard powder diffraction files provided by International Centre for Diffraction Data (ICDD) are used to index the diffraction data obtained from XRD.

3.4.2. Physical parameters

3.4.2.1. Density Measurements

Archimedes principle is used to measure density of as prepared glass samples using microbalance with distilled water as buoyant. Density data obtained is further used to calculate molar volume (V_m) of glasses using the following equation:

$$V_m = \frac{M}{\rho} \tag{3.1}$$

Where M is mass of as prepared glass sample and ρ is the density.

3.4.3. Drug loading

For the loading, doxorubicin hydrochloride (DOX), vancomycin hydrochloride (VANCO), Ibuprofen (IBP) and amoxicillin (AMX) drugs were loaded into mesoporous glasses. For loading of drugs, DOX, VANCO, IBP, AMX were firstly dissolved in ultrapure water with concentrations at 20, 40, 60, 80 and 100 µg/ml. 50 mg of each MBG is then dissolved in 4 ml of ultrapure solutions of DOX, VANCO, IBP and AMX, further these mixtures were kept on shaking for 24 h. To separate the contents of mixtures i.e. supernatant and MBG, after shaking, all mixtures were centrifuged at 2000 rpm for 25 min. UV analysis was used to record the loading efficiency of MBGs and for this, firstly DOX, VANCO, IBP and AMX concentrations were calculated before and after loading in loading medium. The loading of MBGs were recorded at room temperature with ultrapure water as reference using UV spectrophotometer (Model: Hitachi 3900H) in the wavelength range of 200–800 nm.

3.4.3.1. UV- Visible spectroscopy

It tells about the spectroscopy of photons in the UV-Visible region. Light used here is in visible and adjacent near ultraviolet (UV) and near infrared (NIR) ranges. Molecules undergo electronic transitions in the region of electromagnetic spectrum. For the analysis of sample absorption,

transmission and emission of ultraviolet and visible wavelength, UV-visible is the reliable and accurate procedure. Absorption and transmission of electromagnetic radiations by atoms or molecules are measured by UV spectroscopy (Model: Hitachi 3900H). In present study, a double beam of UV with wavelength in the range of 200-800 nm is used to record optical absorbance spectra of loaded drugs. Ultrapure distilled water is taken as the reference solution. Spectrum of each sample is normalized to spectrum of the ultrapure water.

3.4.4. Brunauer Emmett Teller (BET) Analysis

It can be used to measure specific surface area of testing material. A fully automated analyzer is used to measure nitrogen multilayer adsorption as function of relative pressure to evaluate precise specific surface area of the material. To determine total surface area, external area and pore area are evaluated by this technique. The external area and pore area evaluated yields the information regarding particle size and surface porosity, which is required for many applications. N_2 gas adsorption-desorption isotherm is used to determine the pore volume, pore size and specific surface area of bioactive glasses with the help of BET analysis (Microtrac BEL, Japan). Before every measurement, reduced pressure at 200^o C for 15 h was used to degas samples.

3.4.5. Cytotoxicity assay

The humun osteosarcoma cell line MG63 was maintained on Dulbecco's modified Eagle;s medium (DMEM) with streptomycin (100 µg ml^{-1}), gentamycin (100 µg ml^{-1}) and 10% fetal bovine serum (sigma – Aldrich) as supplement at 37º C in humid environment containing 5% CO_2. The cell integrity and potential cytotoxicity extract was assessed by monitoring the uptake of a vital dye 3-(4,5-Dimethylthiazol-2-yl)-5-(3-carboxymethoxyphenyl)-2-(4-sulfophenyl)-2H-tetrazolium (MTS). Including untreated control samples, each sample was pipetted in 9 wells of a 96 well plate in triplicate at desired concentrations, as given below to a total volume of 200 µl. A 500 µl volume of lymphocyte suspension at a concentration of 2×10^4 cells ml^{-1} was added to each well. Then the incubation of the plate was done at 37ºC, 5% CO_2 in air and 90% relative humidity in CO_2 incubator for 72 h. The cells were exposed to all the samples at the glass particle concentrations of 500, 250, 125, 62.5, 31.25, 15.625 and 7.8125 µg/ml for 72 h before adding the MTS assay solution and then incubated for 1-4 hours before taking a reading. After 4 hours, 500 µl of Dimethyl sulfoxide (DMSO) was added to each well. The bluecolored formazan formed was read at 570 nm with Elisa plate reader intriplicate.

CHAPTER-4

RESULTS AND DISCUSSIONS

4.1.General

In this chapter, we will discuss about the results that we obtained from various characterizations. Along with this, behavior and nature of as prepared glass samples will be discussed.

4.2. X-Ray diffraction (XRD) of as prepared glasses

XRD pattern of the as prepared glasses is shown in figure 4.1. It clearly shows the amorphous nature of glass. Absence of Bragg's diffraction peaks clearly indicates that crystalline phases are absent. As prepared glasses exhibit halo peaks in between 15-20^{o}.

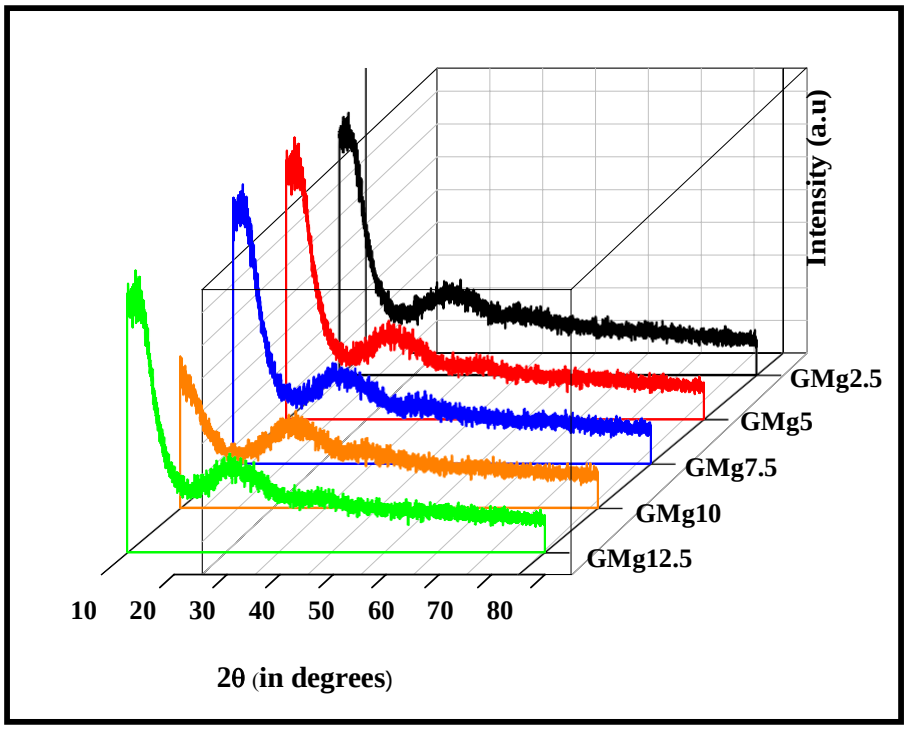

Figure 4.1: XRD spectra of the as prepared glasses**.**

4.3. X-Ray diffraction (XRD) of the heat treated glasses

The XRD pattern of the glass-ceramics (heat treated at 600^{o} C for 72 hr) has been shown in figure 4.2. It clearly reveals information about the crystalline nature of glass after the specified

heat treatment. As Bragg's diffraction peaks are present, hence it implies that different crystalline phases are fomed.

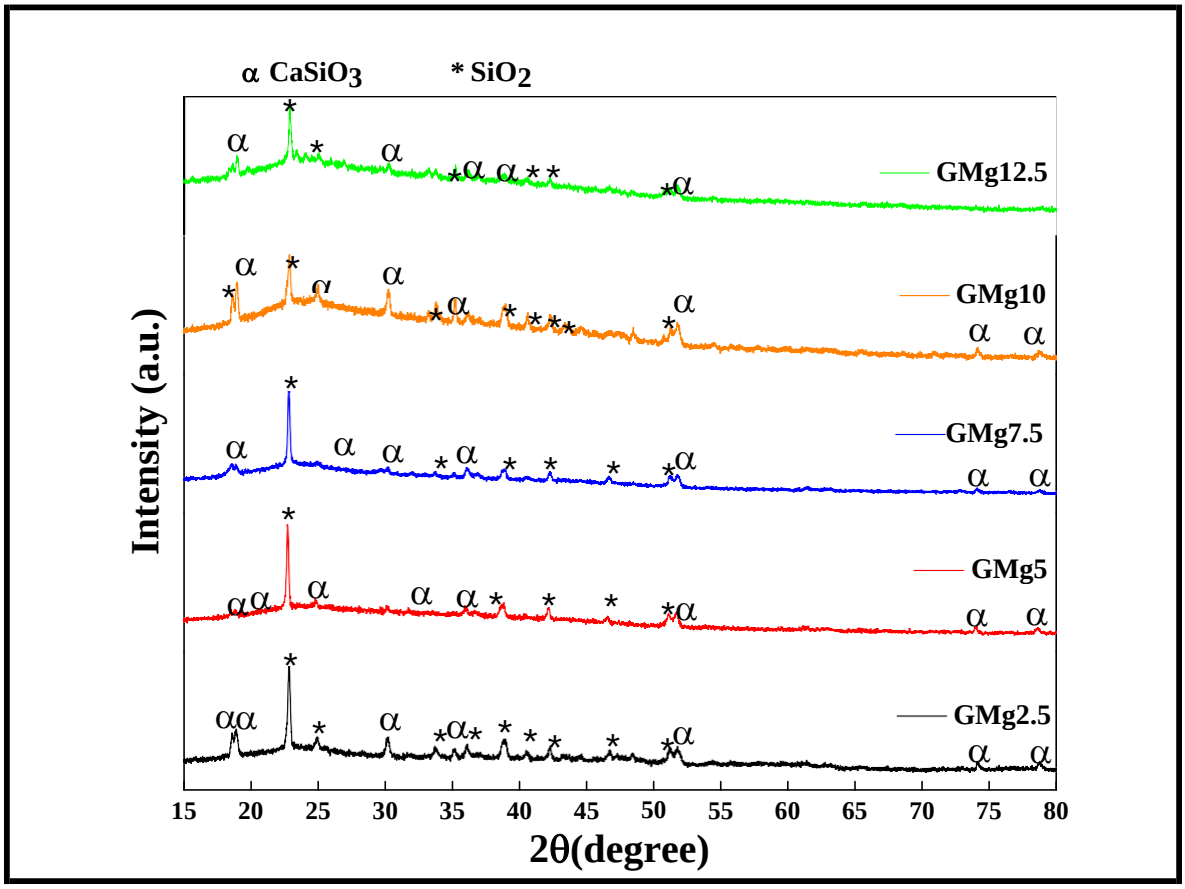

Figure 4.2: XRD spectra of the as prepared bio glass-ceramics.

The XRD patterns of all the as prepared glass- ceramics indicates the presence of crystalline phase of silicon oxide (SiO_2, card number: 01-079-0563) and calcium silicate ($CaSiO_3$, card number: 01-072-2284). The reaction mechanism can be given as:-

$$CaO + SiO_2 \longrightarrow CaSiO_3 \qquad (4.1)$$

It is depicted from fig 4.2. that with the increase in magnesium content, the SiO_2 phase gets suppressed. Moreover, the $CaSiO_3$ phase is also suppressed. This indicates more SiO_2 is engaged in network formation.

4.4. Physical parameters (density & molar volume) of glass samples

The as prepared samples were analyzed for the density and molar volume. With decreasing copper content in glass samples, molar mass vary from 70.82 to 66.90 g. Moreover, molar volume of these glass samples varies from 47.80 to 51.06 cm^3. The density values are listed in Table 4.1. respectively.

Table 4.1: Molar mass, Molar volume and density of prepared samples

Sample name	Molar Mass(M) (g)	Molar Volume(V_m) (cm^3)	Density (g/cm^3)
GMg2.5	70.82	47.80	1.48
GMg5	69.84	47.83	1.46
GMg7.5	68.85	48.48	1.42
GMg10	67.88	50.65	1.34
GMg12.5	66.90	51.06	1.31

Molar mass of the samples decreased with increasing magnesium and decreasing copper content and varies as follow:-

GMg2.5>GMg5>GMg7.5>GMg10>GMg12.5 (Table 4.1)

With increasing Mg content, the density shows decreasing trend. Copper is heavier than Magnesium and hence the density of 1.48 g/cm^3 is maximum for the GMg2.5 MBG i.e GMg2.5 contains 12.5 % CuO.

4.5. BET Analysis

The parameters obtained from BET i.e. pore volume, surface area and pore-size are listed in Table 4.2. Surface are of these samples varied from 104.37 to 41.307 cm^2/g range. BET analysis showed that, upto GMg5 surface area of samples increases from 219.69 to 442.41 cm^2/g and then with the increase in magnesium content, surface area decreases from 104.37 to 41.307 cm^2/g. In addition to this, pore volume of glass samples varied from 0.0830 to 0.6029 cm^3/g. Nitrogen sorption isotherms obtained from all the glass samples presented a typical IV isotherm pattern indicating that they are mesoporous materials as shown in fig 4.3. The mesopore pore size

distribution of all the glass samples lies in the range of 5.8-8.8 nm as shown in fig 4.4. Glass is regarded as MBG for pore size of 2-50 nm [1-3].

Table 4.2: Pore volume, Surface area and Pore size of prepared samples

Sample name	Pore Volume (cm^3/g)	Surface Area (cm^2/g)	Pore Size (nm)
GMg2.5	0.3917	219.69	8.4
GMg5	0.6029	442.41	5.8
GMg7.5	0.1741	104.37	7.2
GMg10	0.1481	98.22	6.7
GMg12.5	0.0830	41.307	8.8

Along with this, pore volume, surface area and pore size of pores were measured with BET analysis. BET analysis showed that, upto GMg5 surface area of samples increases from 219.69 to 442.41 cm^2/g and then with the increase in magnesium content, surface area decreases from 104.37 to 41.307 cm^2/g. In addition to this, pore volume of glass samples varied from 0.0830 to 0.6029 cm^3/g. Nitrogen sorption isotherms obtained from all the glass samples presented a typical IV isotherm pattern indicating that they are mesoporous materials as shown in fig 4.3. The mesopore pore size distribution of all the glass samples lies in the range of 5.8-8.8 nm as shown in fig 4.4.

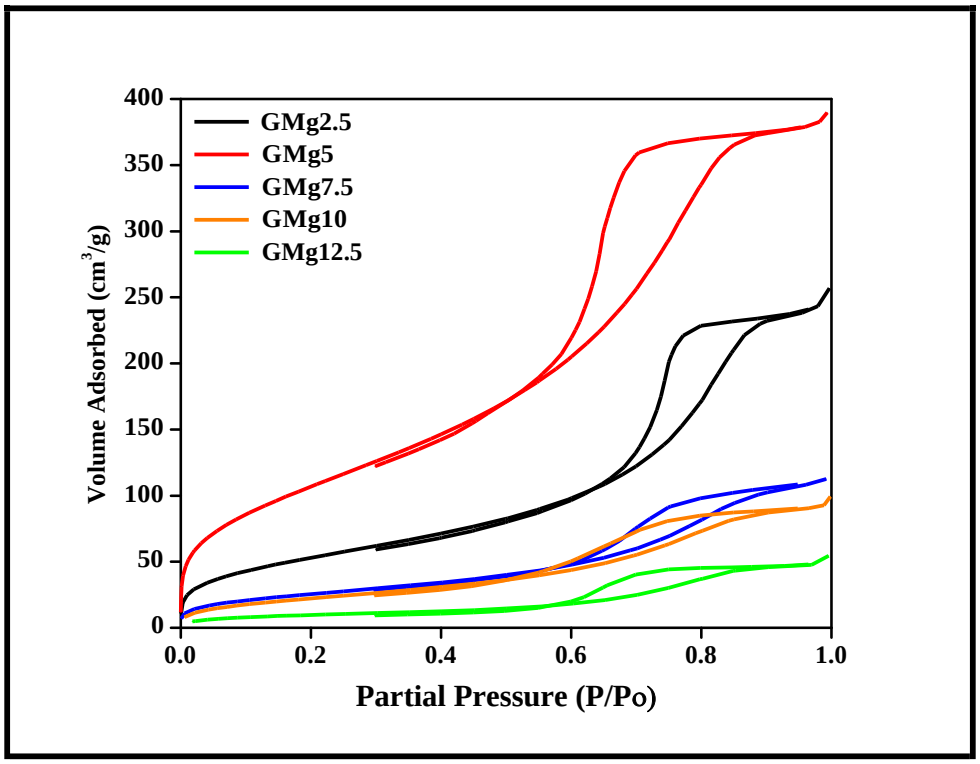

Fig.4.3: Nitrogen-adsorption-desorption isotherm

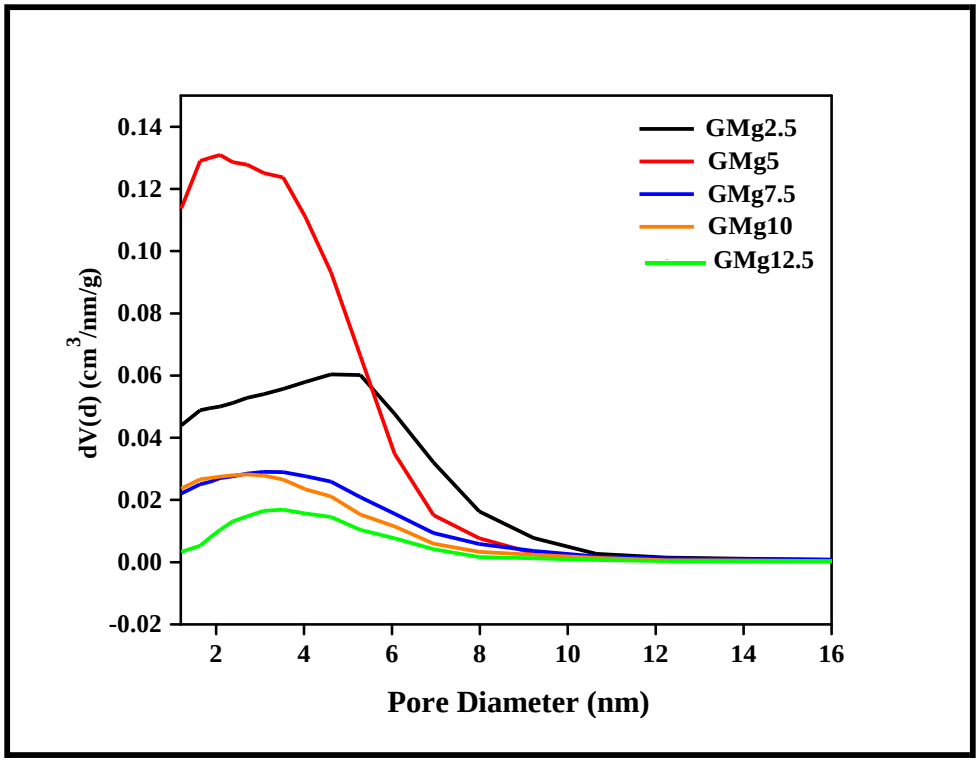

Fig. 4.4: Mesopore pore size distribution

4.6. Calibration Curves for the drugs

Standard drug solutions of concentrations ranging from 20-100 µg/ml were prepared. UV visible spectrophotometer is used to create a calibration curve analyzing absorbance of different drugs at different concentrations. The drug loading efficiency is determined by measuring the concentration of drug left behind in the supernatant and is calculated from the slope of the calibration curve. The calibration curve of VANCO, DOX, IBP and AMX at concentrations 20, 40, 60, 80 and 100 µg/ml as shown in fig 4.5 (a-d) respectively with their slopes are given below:

Slope of VANCO - $Y = 124.7x - 0.020$, $R^2 = 0.976$ (4.2)

Slope of DOX - $Y = 0.001x - 0.003$, $R^2 = 0.991$ (4.3)

Slope of IBP - $Y = 132.2x - 0.133$, $R^2 = 0.932$ (4.4)

Slope of AMX- $Y = 0.010x - 0.251$, $R^2 = 0.920$ (4.5)

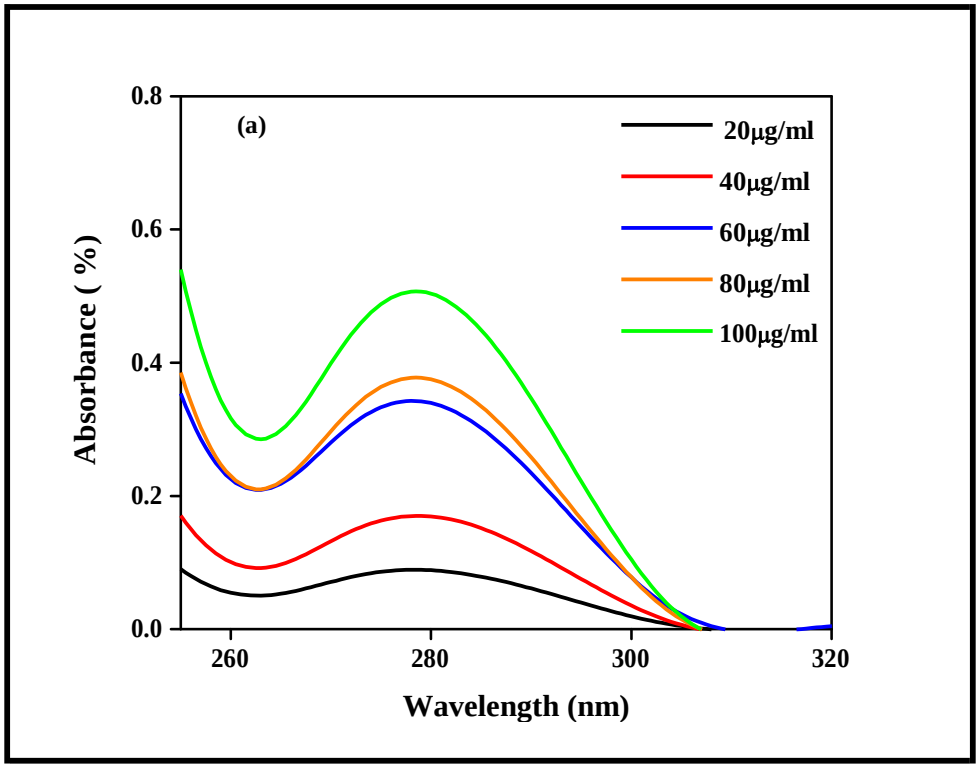

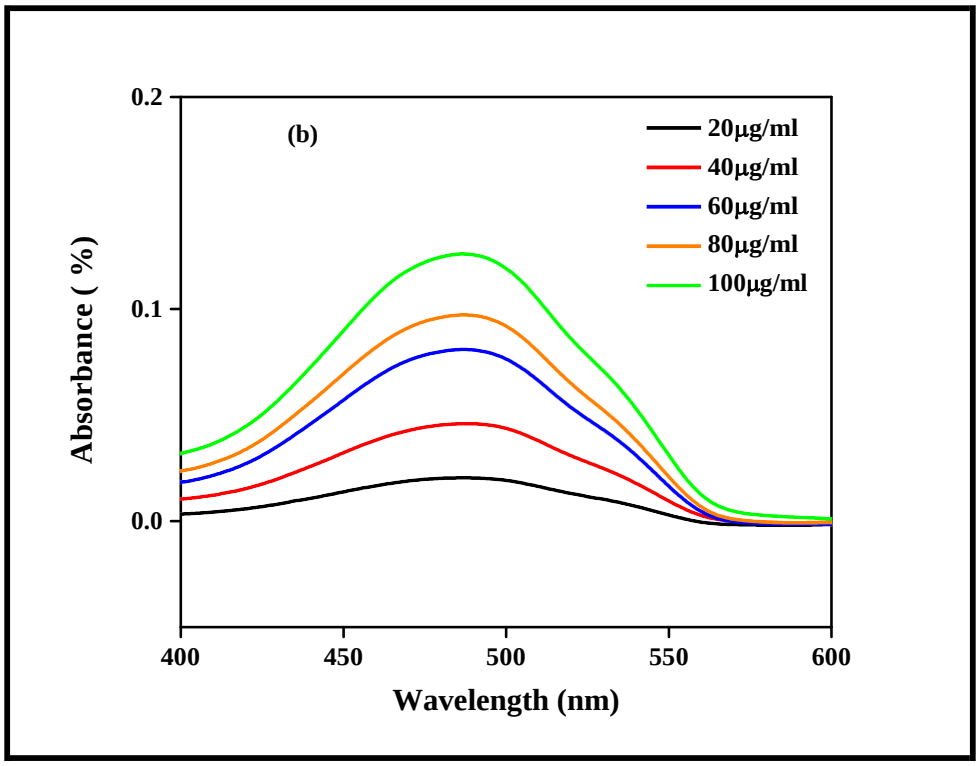
(b)
20µg/ml
40µg/ml
60µg/ml
80µg/ml
100µg/ml
Absorbance (%)
0.2
0.1
0.0
400
450
500
550
600
Wavelength (nm)

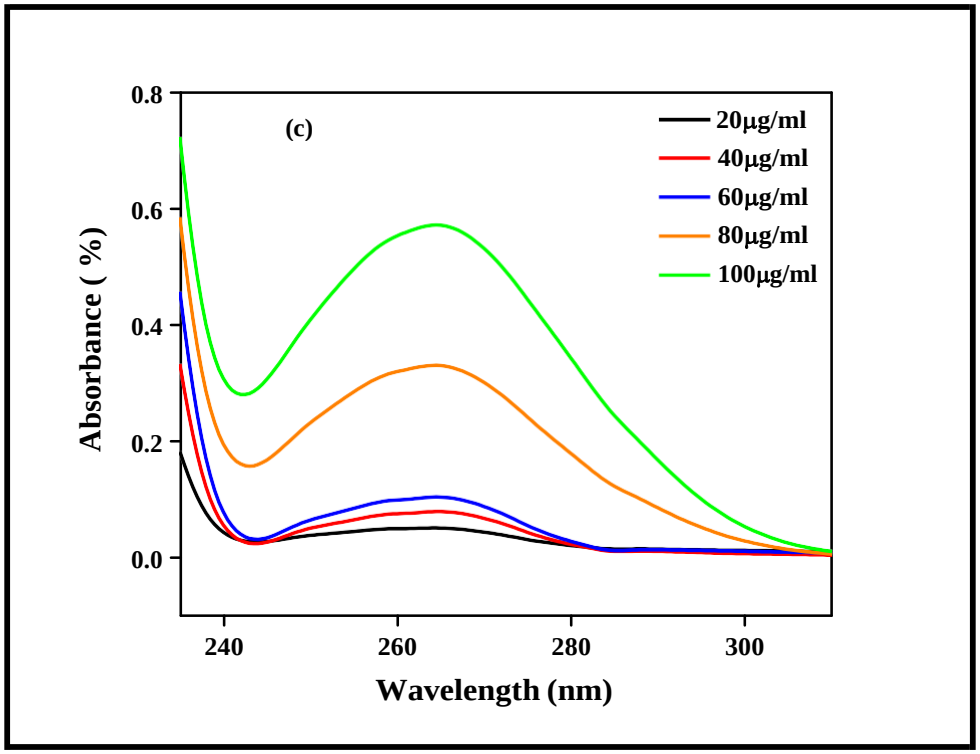
(c)
20µg/ml
40µg/ml
60µg/ml
80µg/ml
100µg/ml
Absorbance (%)
0.8
0.6
0.4
0.2
0.0
240
260
280
300
Wavelength (nm)

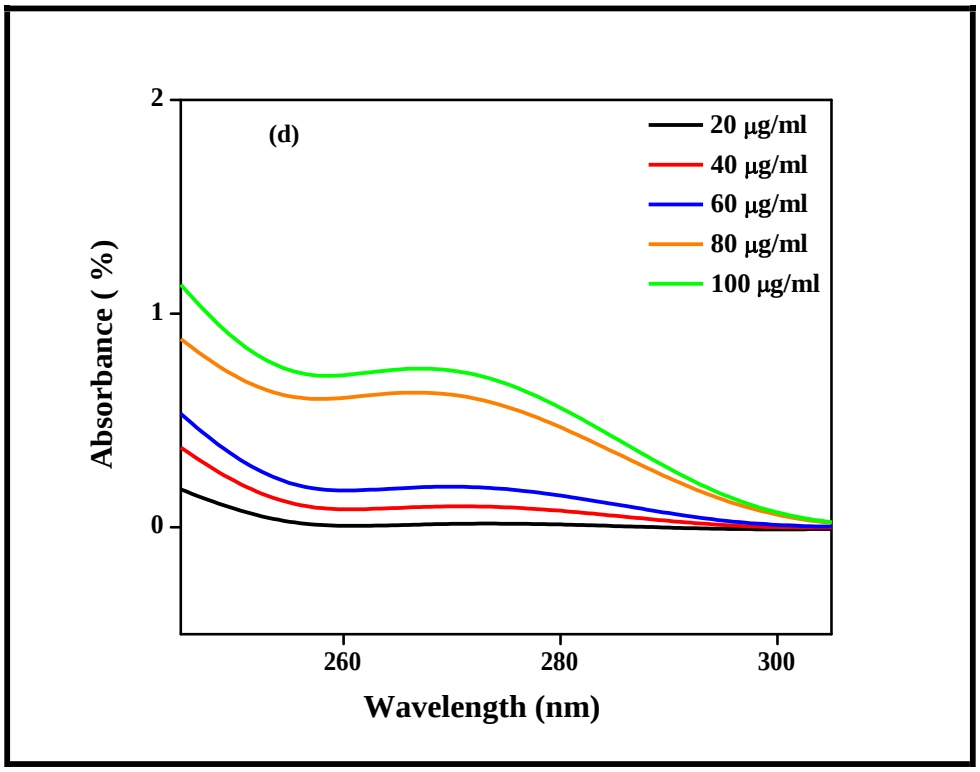

Fig 4.5: Calibration curves of (a) VANCO, (b) DOX, (c) IBP and (d) AMX respectively.

4.7. Drug loading kinetics

To determine drug release profile, all the glass samples were immersed in a highly concentrated drug solution. The samples are loaded with different amount of drugs. In present study, four drugs have been loaded separately in the mesoporous glass matrix. These drugs are vancomycin (VANCO), doxorubicin (DOX), Ibuprofen (IBP) and amoxicillin (AMX). These are loaded at different concentrations at 20, 40, 60, 80 and 100 µg/ml in deionized water. The concentration of drugs loaded in the mesoporous glasses is analyzed from the amount of drugs remaining in the supernatant and calibration curves. The drug loading efficiency is given in table 4.3, 4.4, 4.5 and 4.6., respectively.

Table 4.3: Drug loading efficiency (%) of glass samples for VANCO at different concentrations.

Glass sample	VANCO Drug Concentration (µg/ml)				
	20	**40**	**60**	**80**	**100**
GMg2.5	100	100	0	0	0
GMg5	100	100	0	0	0
GMg7.5	100	100	0	0	0
GMg10	100	100	0	0	0
GMg12.5	100	100	0	0	0

In all the glass samples, the loading behavior of the drug VANCO was found to be 100% at 20 and 40 µg/ml concentrations, while at another concentrations (60, 80 and 100 µg/ml), VANCO was not loaded in the glass samples.

Table 4.4: Drug loading efficiency (%) of glass samples for DOX at different concentrations.

Glass sample	DOX Drug Concentration (µg/ml)				
	20	**40**	**60**	**80**	**100**
GMg2.5	100	55	32	20	0
GMg5	100	61	27	14	0
GMg7.5	100	61	19	17	0
GMg10	100	56	23	18	0
GMg12.5	79	63	31	19	0

However, DOX had highest loading at 20 µg/ml concentrations (100%) except for sample GMg12.5, which shows loading of about 79%. And with increasing concentration of drug,

loading was decreased from 100 to 14% in case of DOX. At 100 µg/ml, DOX was not loaded in any of the glass samples.

Table 4.5: Drug loading efficiency (in %) of glass samples for IBP at different concentrations.

Glass sample	IBP Drug Concentration (µg/ml)				
	20	**40**	**60**	**80**	**100**
GMg2.5	100	100	100	100	100
GMg5	100	100	100	100	100
GMg7.5	100	100	100	100	100
GMg10	100	100	100	100	100
GMg12.5	100	100	100	100	100

Table 4.6: Drug loading efficiency (in %) of glass samples for IBP at different concentrations.

Glass sample	AMX Drug Concentration (µg/ml)				
	20	**40**	**60**	**80**	**100**
GMg2.5	100	100	100	100	100
GMg5	100	100	100	100	100
GMg7.5	100	100	100	100	100
GMg10	100	100	100	100	100
GMg12.5	100	100	100	100	100

In all the glass samples, IBP and AMX drug was loaded fully for all the concentrations. The loading of all the drugs in different glass samples as bar graphs are shown in fig 4.6, 4.7, 4.8, 4.9 and 4.10., respectively.

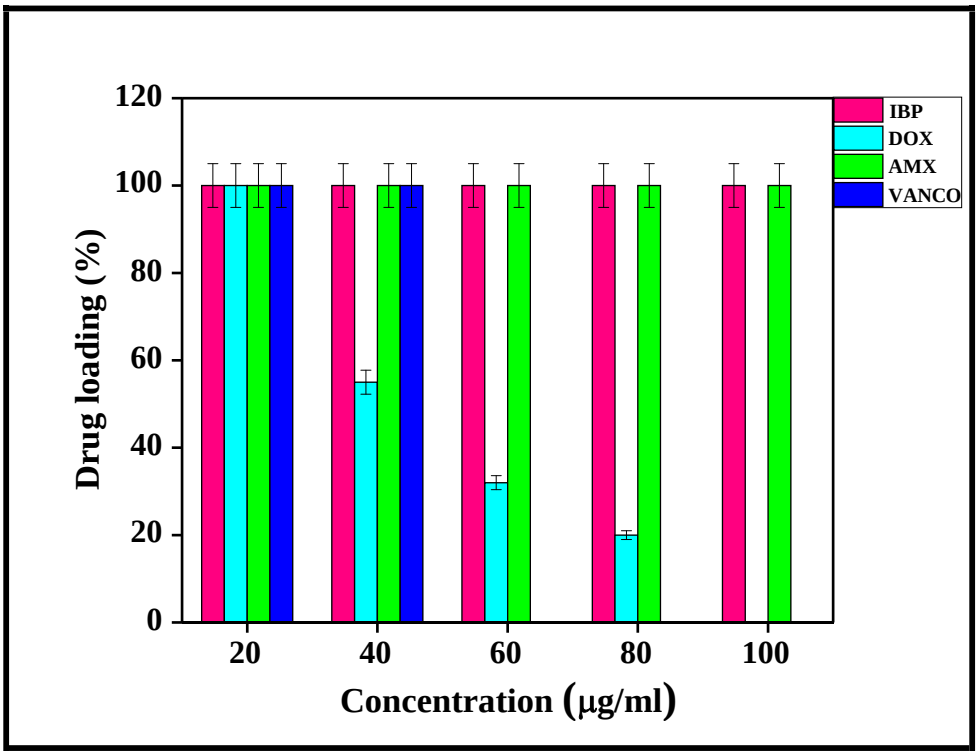

Fig 4.6: Drug loading efficiency of glass sample GMg2.5 for IBP, DOX and AMX at different concentrations.

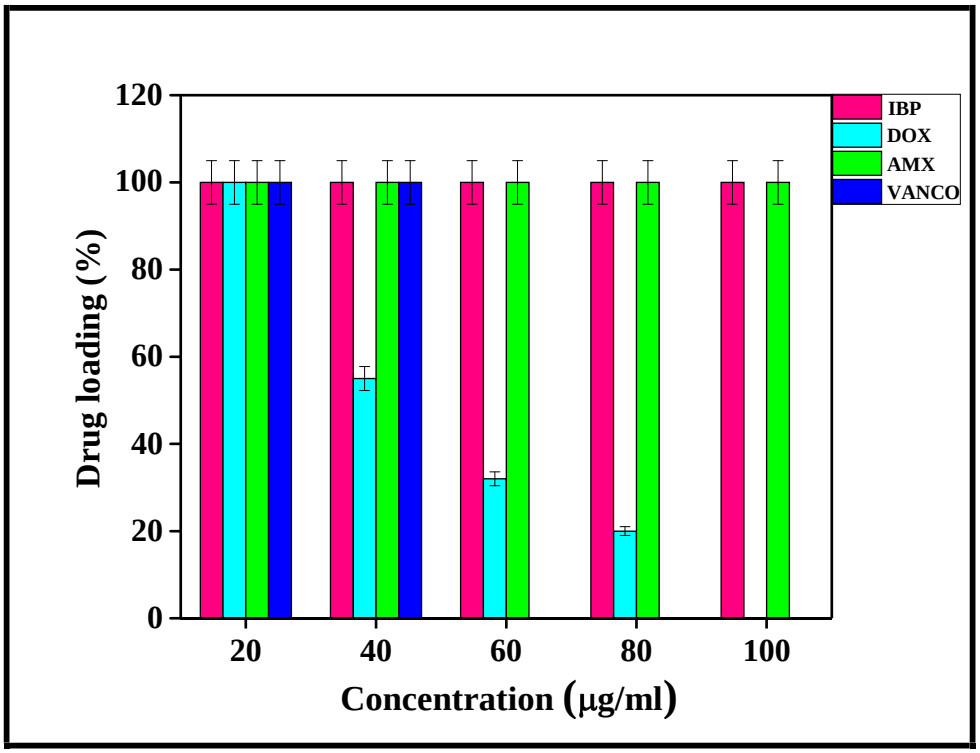

Fig 4.7: Drug loading efficiency of glass sample GMg5 for IBP, DOX and AMX at different concentrations.

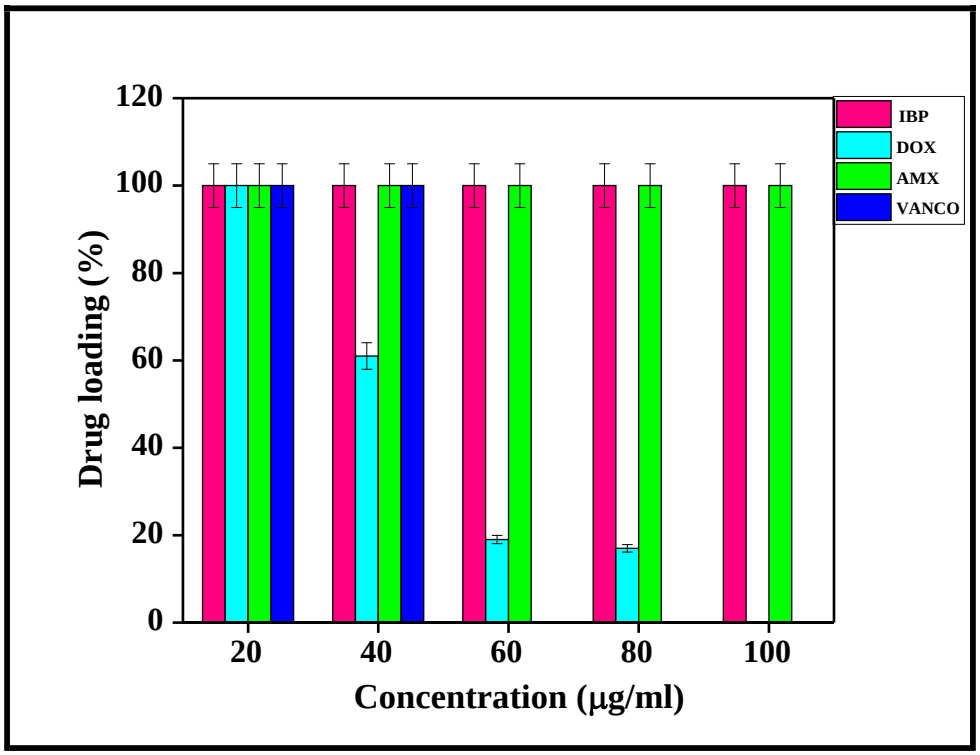

Fig 4.8: Drug loading efficiency of glass sample GMg7.5 for IBP, DOX and AMX at different concentrations.

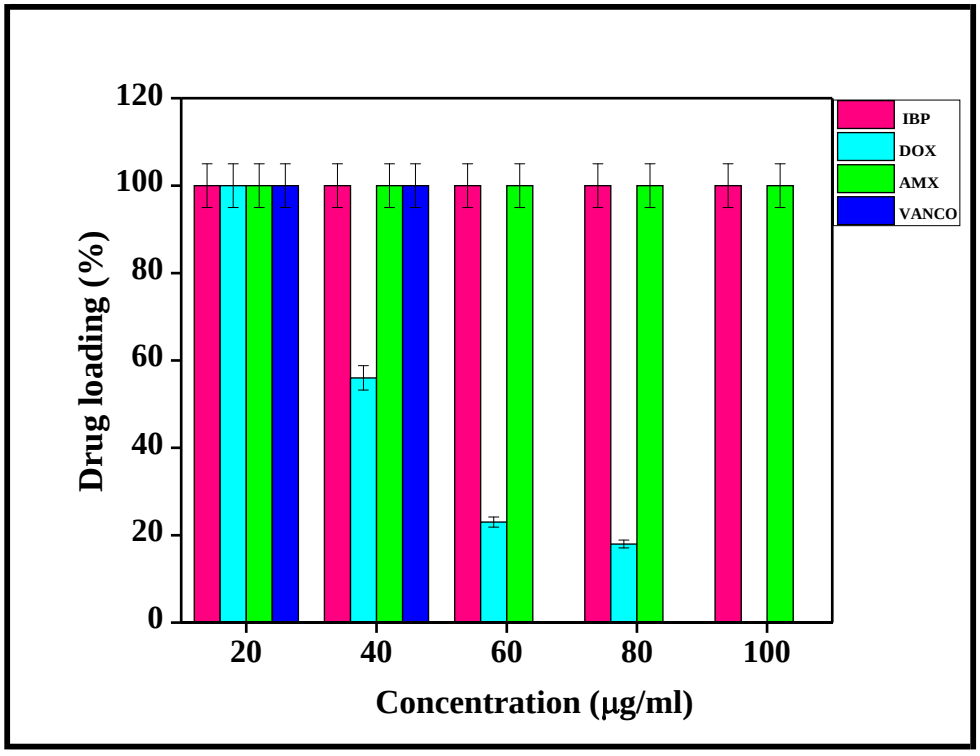

Fig 4.9: Drug loading efficiency of glass sample GMg10 for IBP, DOX and AMX at different concentrations.

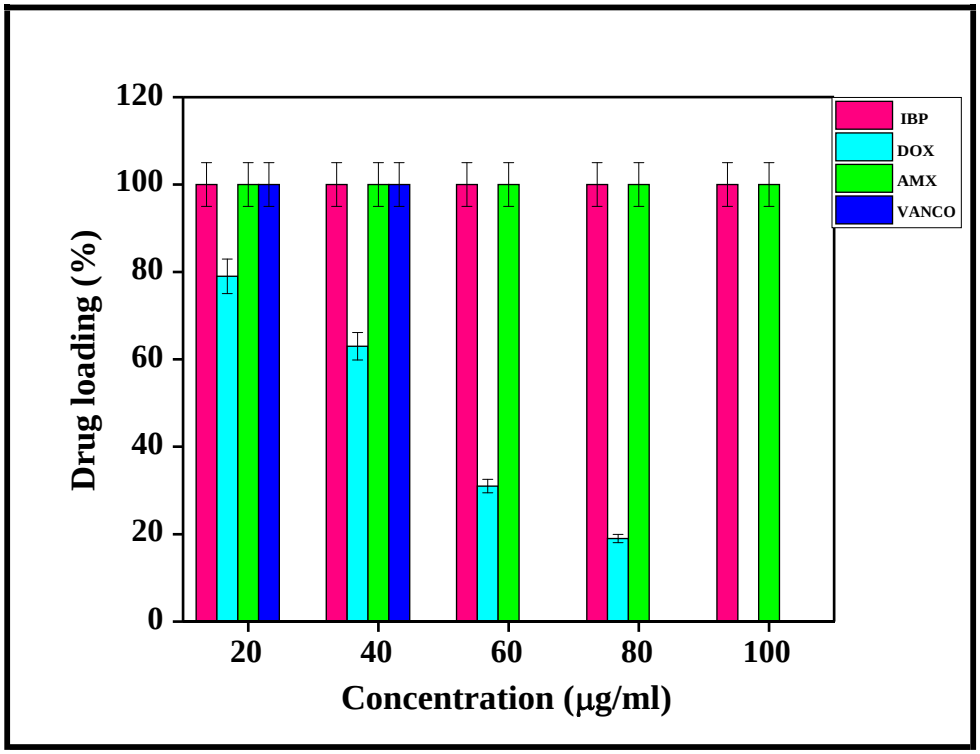

Fig 4.10: Drug loading efficiency of glass sample GMg12.5 for IBP, DOX and AMX at different concentrations.

The UV- absorbance curve for the VANCO loaded MBGs are depicted in fig 4.11 respectively. As VANCO did not yield loading for concentration > 40 μg/ml, hence only 20 and 40 μg/ml loading are given.

4.6.1 VANCO loading

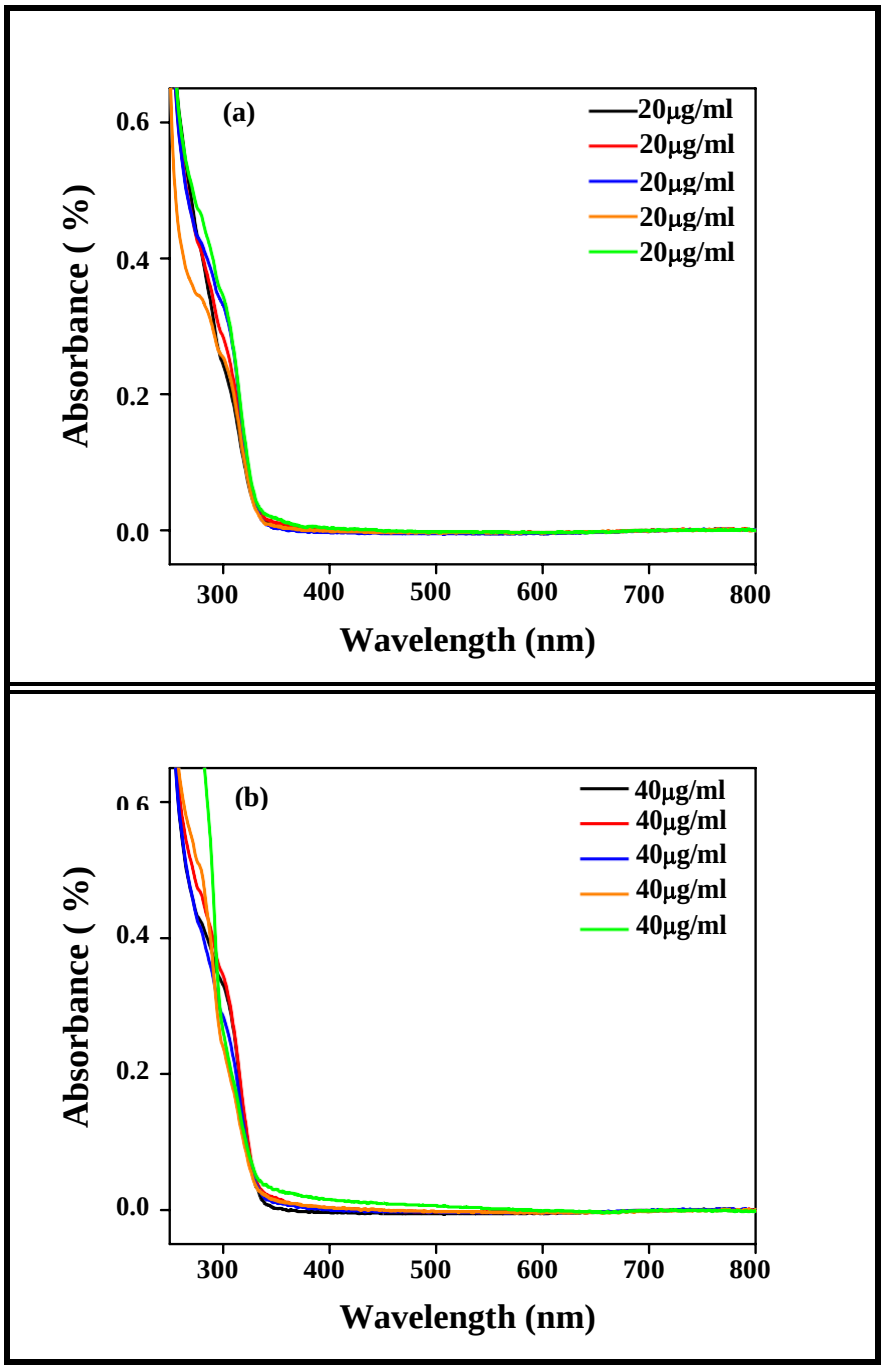

Fig. 4.11: Loading of VANCO in all the mesoporous glasses at concentration (a) 20µg/ml and (b) 40µg/ml.

From the experimental work, it is found that the VANCO is fully loaded in all glass samples at 20 and 40µg/ml concentrations whereas for higher concentrations, VANCO shows no loading. Garg et al. [4] had obtained 100% loading efficiency of VANCO in MBGs.

4.6.2 DOX loading

The loading of DOX at different concentrations for all the MBGs are shown in fig 4.9 (a-e)., respectively.

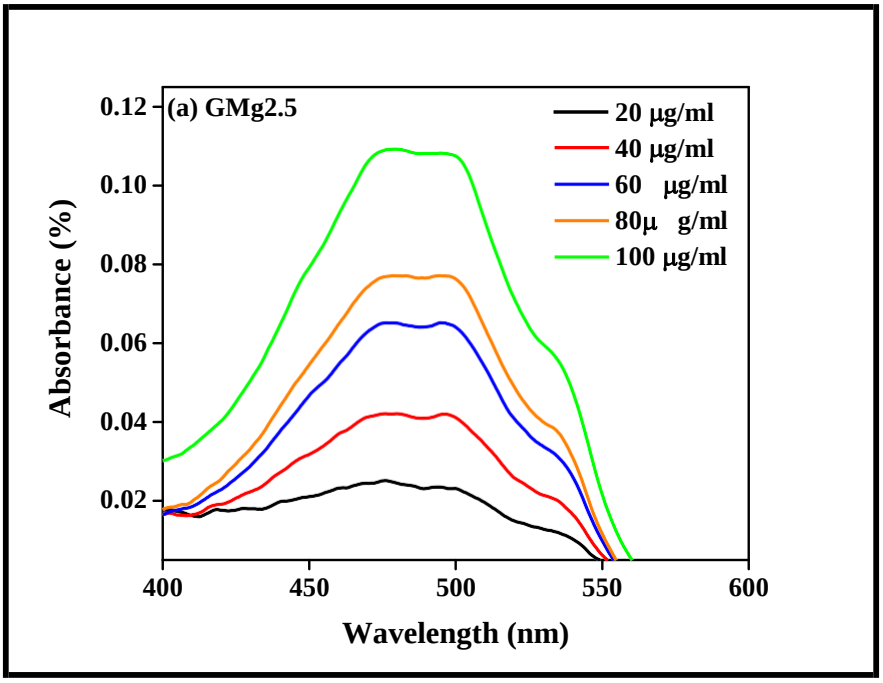

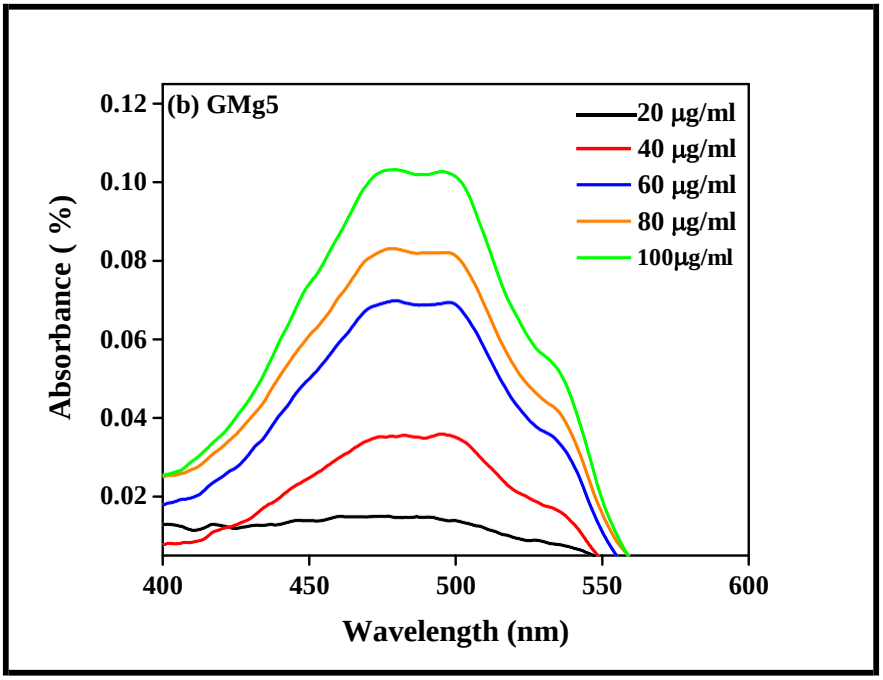

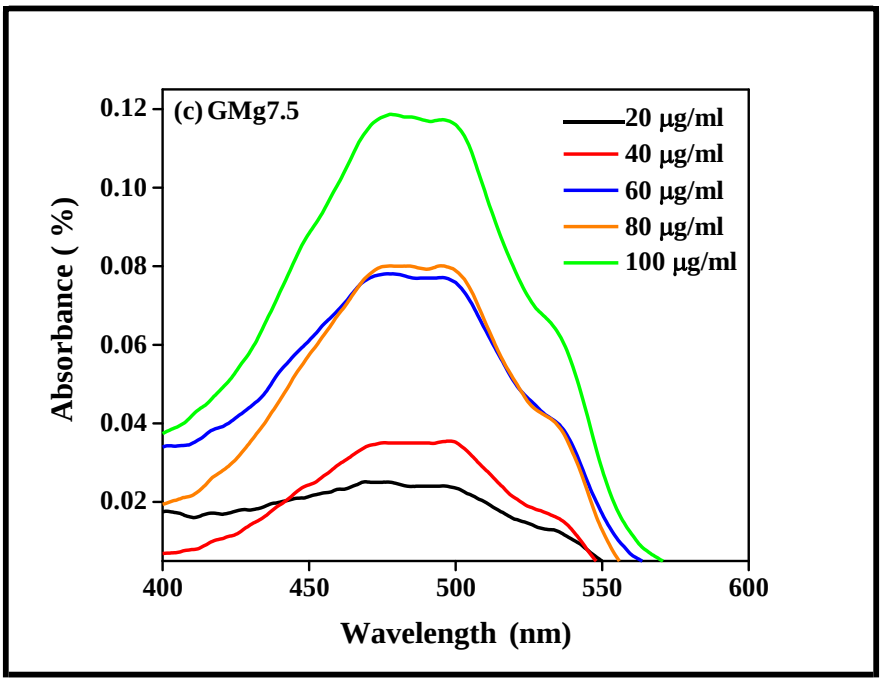
(c) GMg7.5
20 µg/ml
40 µg/ml
60 µg/ml
80 µg/ml
100 µg/ml
Absorbance (%)
0.12
0.10
0.08
0.06
0.04
0.02
400
450
500
550
600
Wavelength (nm)

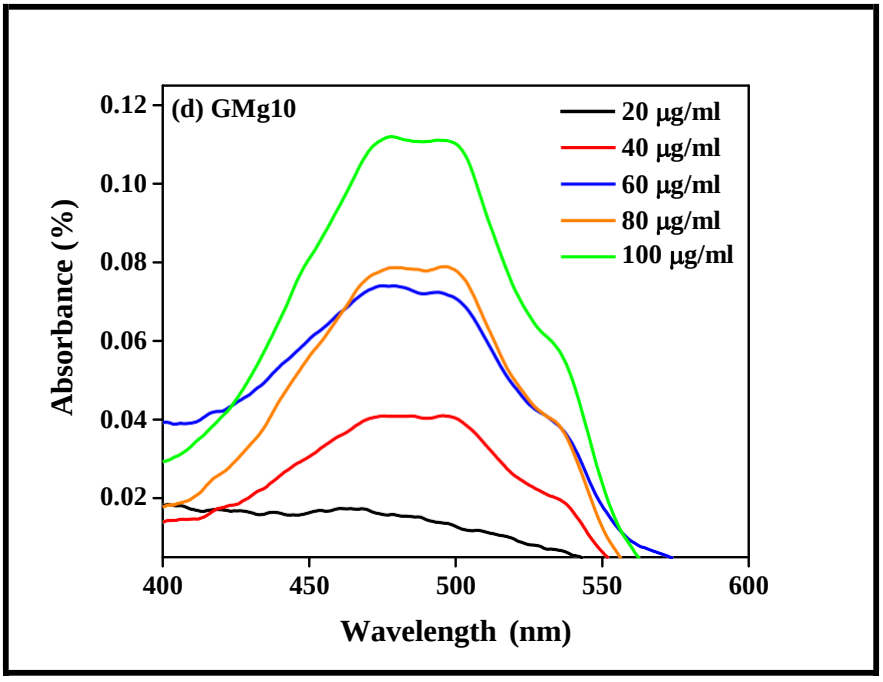
(d) GMg10
20 µg/ml
40 µg/ml
60 µg/ml
80 µg/ml
100 µg/ml
Absorbance (%)
0.12
0.10
0.08
0.06
0.04
0.02
400
450
500
550
600
Wavelength (nm)

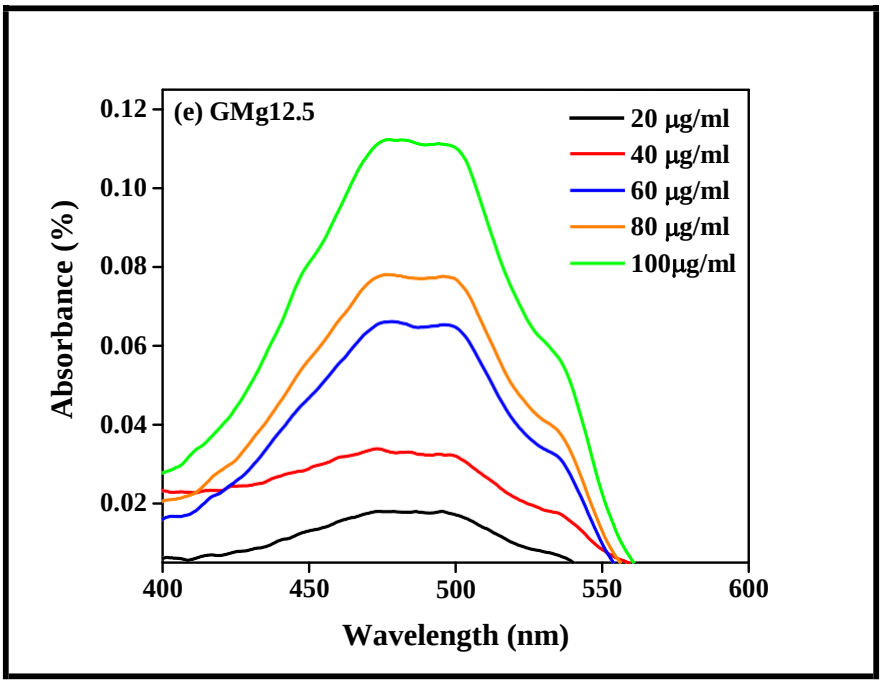

Fig 4.12: Loading of DOX in (a) GMg2.5, (b) GMg5, (c) GMg7.5, (d) GMg10 and (e) GMg12.5 MBGs respectively at different concentrations.

It was evident that in case of DOX, as the concentration of drug is increased, loading decreases and at 100 µg/ml, DOX was not loaded in all the MBGs. For instance, at concentration of 20 µg/ml, for GMg2.5 glass sample, loading is obtained to be 100%. However for the same glass sample, when concentration of drug reached 80 µg/ml, loading decreased to 20%. Similarly, for all other MBGs at different concentrations, loading of drugs varied. For GMg5 glass sample, loading decreased from 100% to 14% with increasing concentrations of the drug. For GMg7.5, loading decreased from 100% to 17% whereas for GMg10 MBG, loading decreased up to 18% from 100%. For GMg12.5, loading varies from 79% to 19%. Garg et al.[4] obtained highest 91.4 % loading for DOX in MBGs whereas our group obtained 100% loading for DOX.

4.6.3 IBP loading

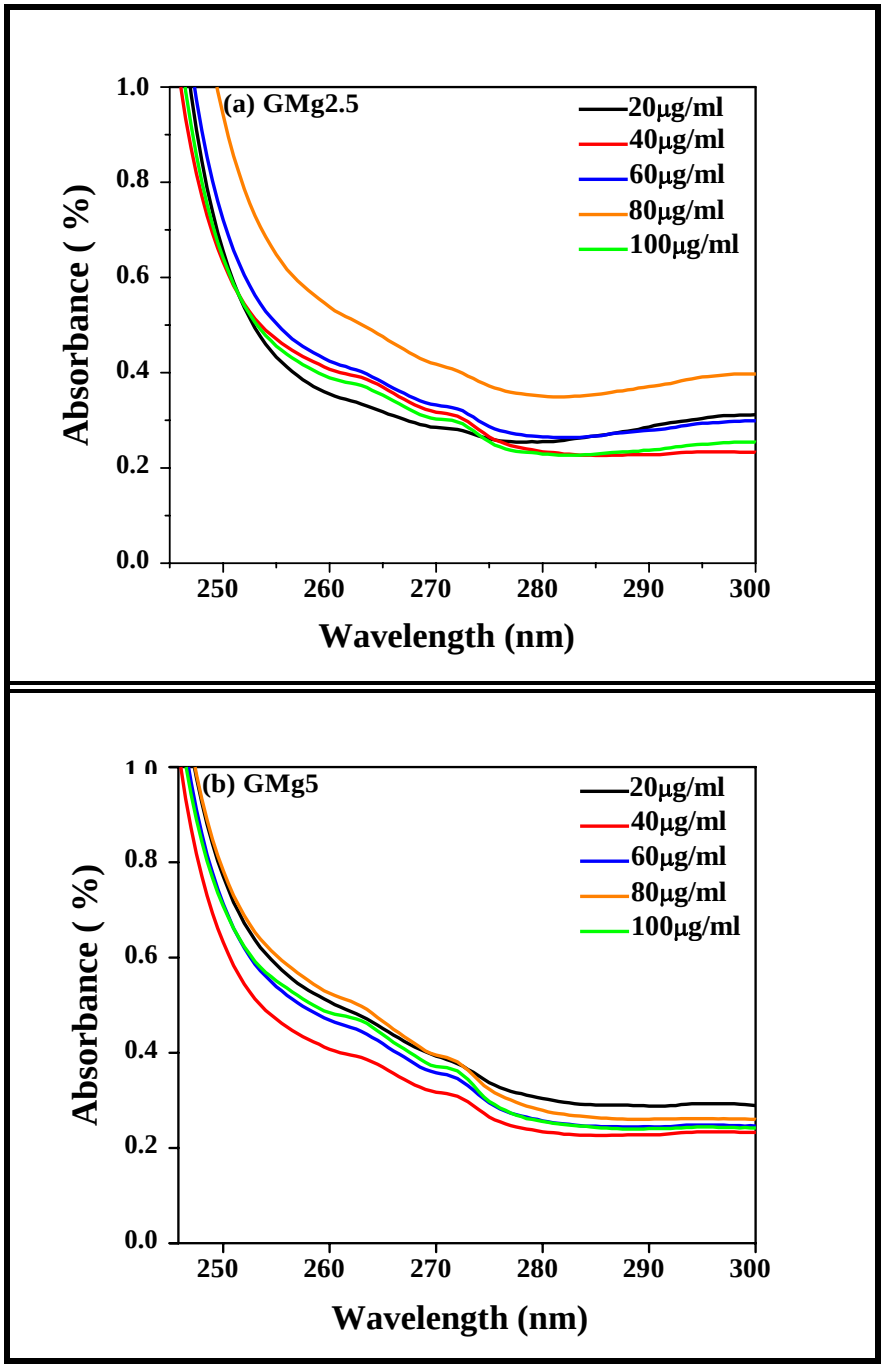

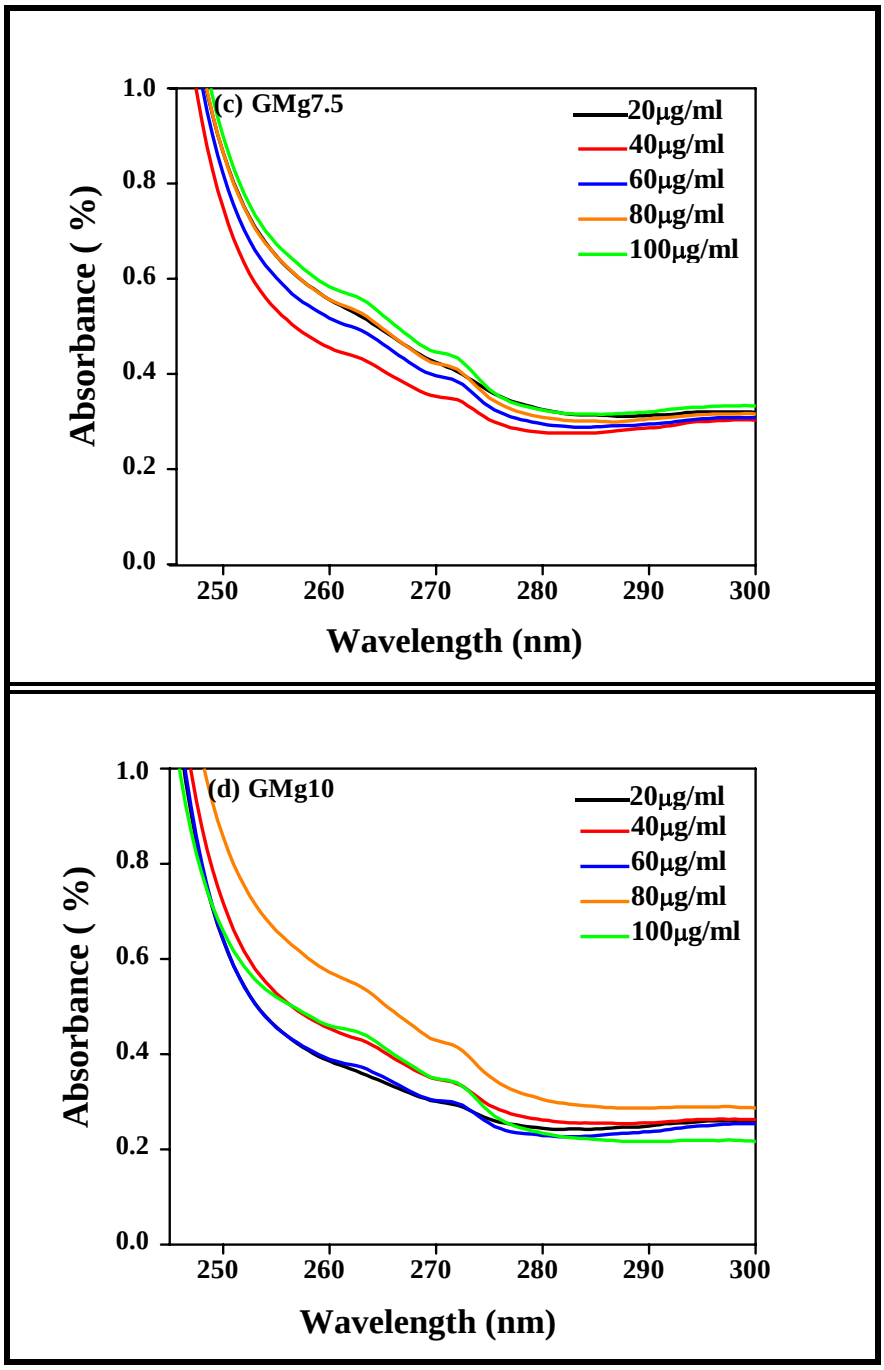
(c) GMg7.5
20µg/ml
40µg/ml
60µg/ml
80µg/ml
100µg/ml
Absorbance (%)
Wavelength (nm)
(d) GMg10
20µg/ml
40µg/ml
60µg/ml
80µg/ml
100µg/ml
Absorbance (%)
Wavelength (nm)

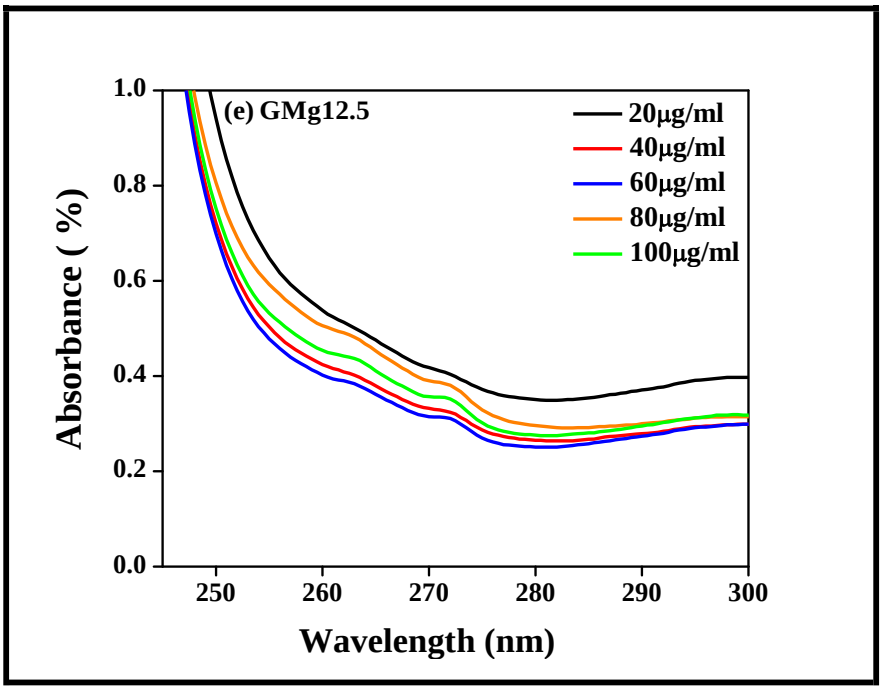

Fig 4.13: Loading of IBP in (a) GMg2.5, (b) GMg5, (c) GMg7.5, (d) GMg10 and (e) GMg12.5 mesoporous glasses respectively at different concentrations.

It was found that IBP was fully loaded in all the MBGs at all the concentrations, hence, indicating that MBGs with decreasing copper and increasing magnesium content are a considerable drug carrier for the IBP drug.

4.6.4 AMX loading

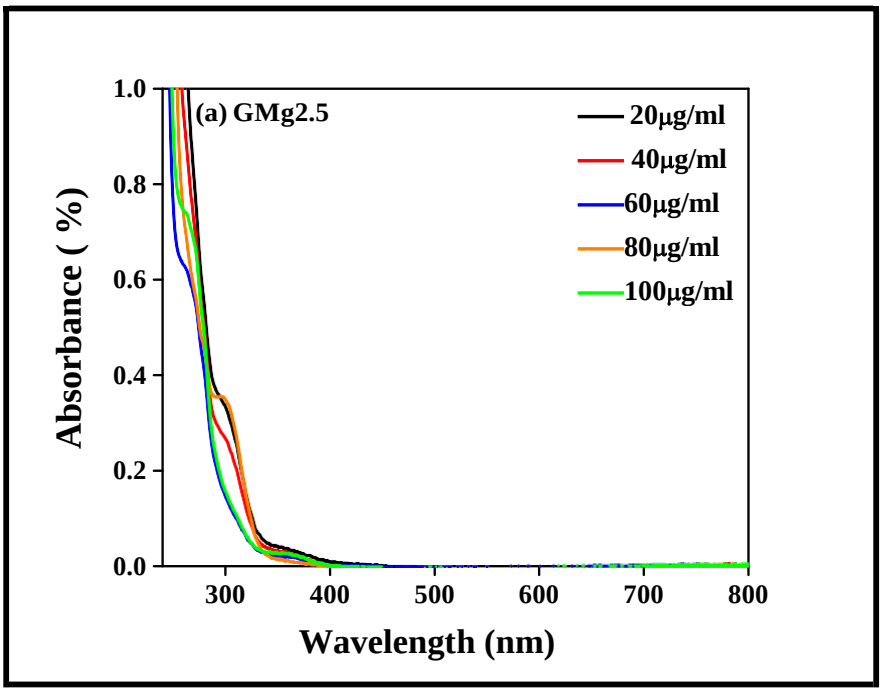
(a) GMg2.5
20µg/ml
40µg/ml
60µg/ml
80µg/ml
100µg/ml
Absorbance (%)
Wavelength (nm)
1.0
0.8
0.6
0.4
0.2
0.0
300
400
500
600
700
800

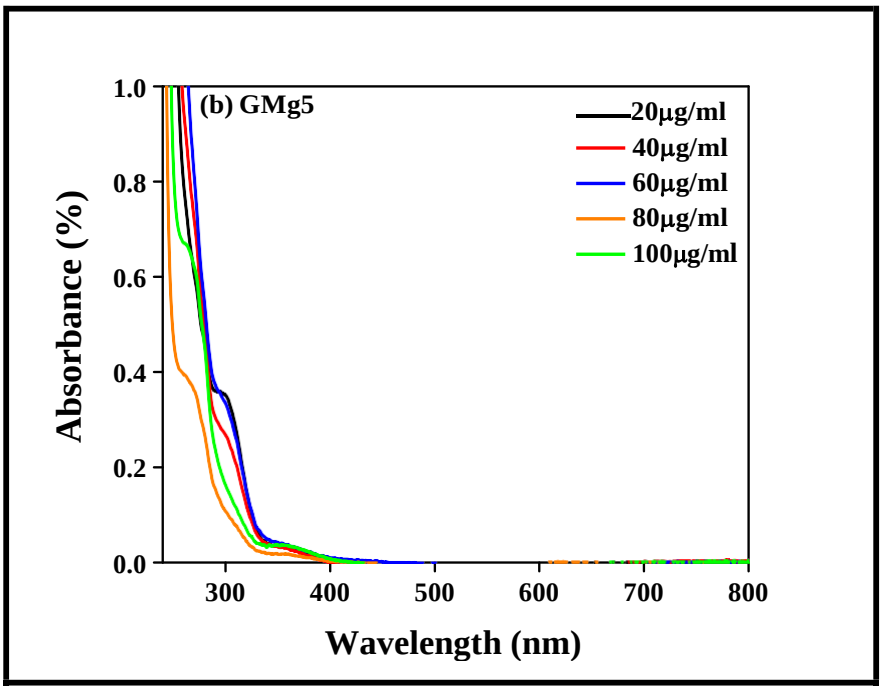
(b) GMg5
20µg/ml
40µg/ml
60µg/ml
80µg/ml
100µg/ml
Absorbance (%)
Wavelength (nm)
1.0
0.8
0.6
0.4
0.2
0.0
300
400
500
600
700
800

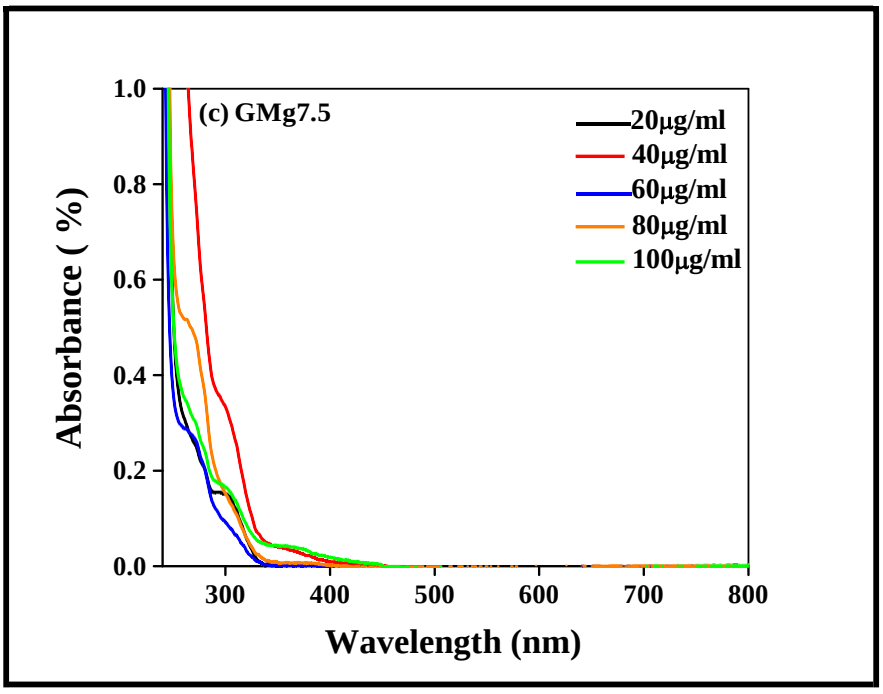
(c) GMg7.5
20µg/ml
40µg/ml
60µg/ml
80µg/ml
100µg/ml
Absorbance (%)
Wavelength (nm)
1.0
0.8
0.6
0.4
0.2
0.0
300
400
500
600
700
800

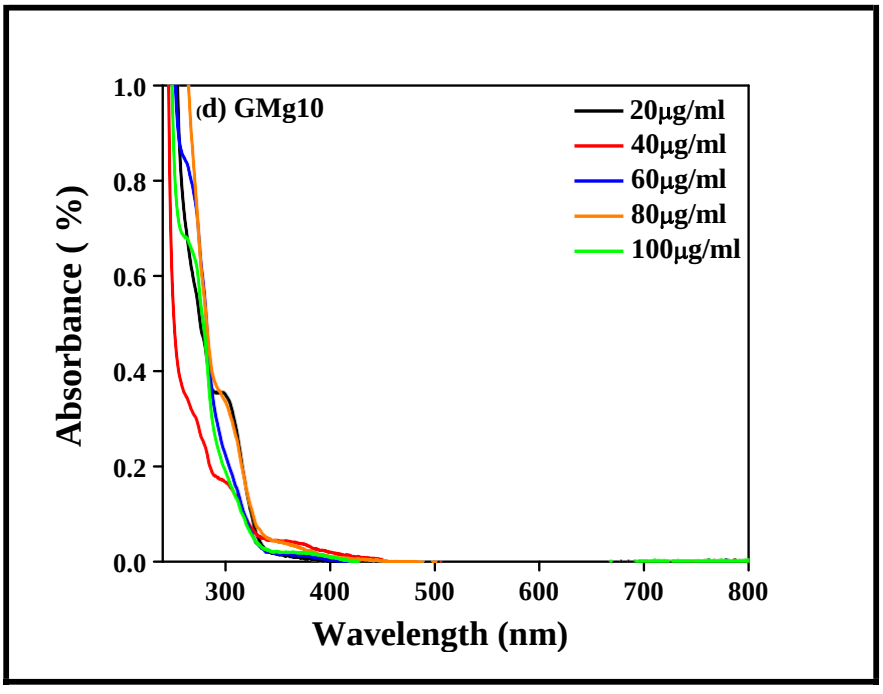
(d) GMg10
20µg/ml
40µg/ml
60µg/ml
80µg/ml
100µg/ml
Absorbance (%)
Wavelength (nm)
1.0
0.8
0.6
0.4
0.2
0.0
300
400
500
600
700
800

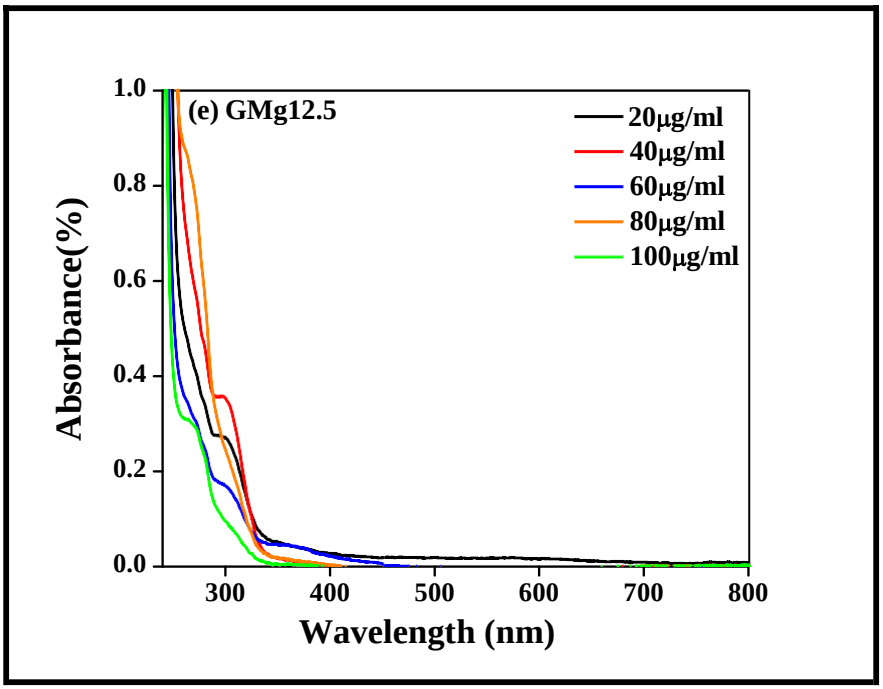

Fig 4.14: Loading of AMX in (a) GMg2.5, (b) GMg5, (c) GMg7.5, (d) GMg10 and (e) GMg12.5 mesoporous glasses respectively at different concentrations.

Similarly as IBP, loading of AMX was also found to be 100% in all the glass samples at all the concentrations, implying that MBGs are more promising condidates for drug loading as compared to BGs.

4.7. Cytotoxicity assays

The MTS assay is colorimetric assay for assessing cell metabolic activity and for determining number of viable cells in proliferation or cytotoxicity assays. It can be used to determine the median toxic dose i.e TD_{50}, which means the dose that causes a toxic response in 50% of the cells which further give accurate results as draws from lethal dose 50 [5]. In the present case, instead of lethal dose, the study is focused at cell proliferation and survival rate. Hence, 100% is taken to be as control and anything, which is below 90% is considered to be toxic [6]. Cytotoxicity is directly linked with the reactivity of the compounds. More the ionic exchange between the environment and the glass particles higher the cytotoxicity due to surface modifications [7].

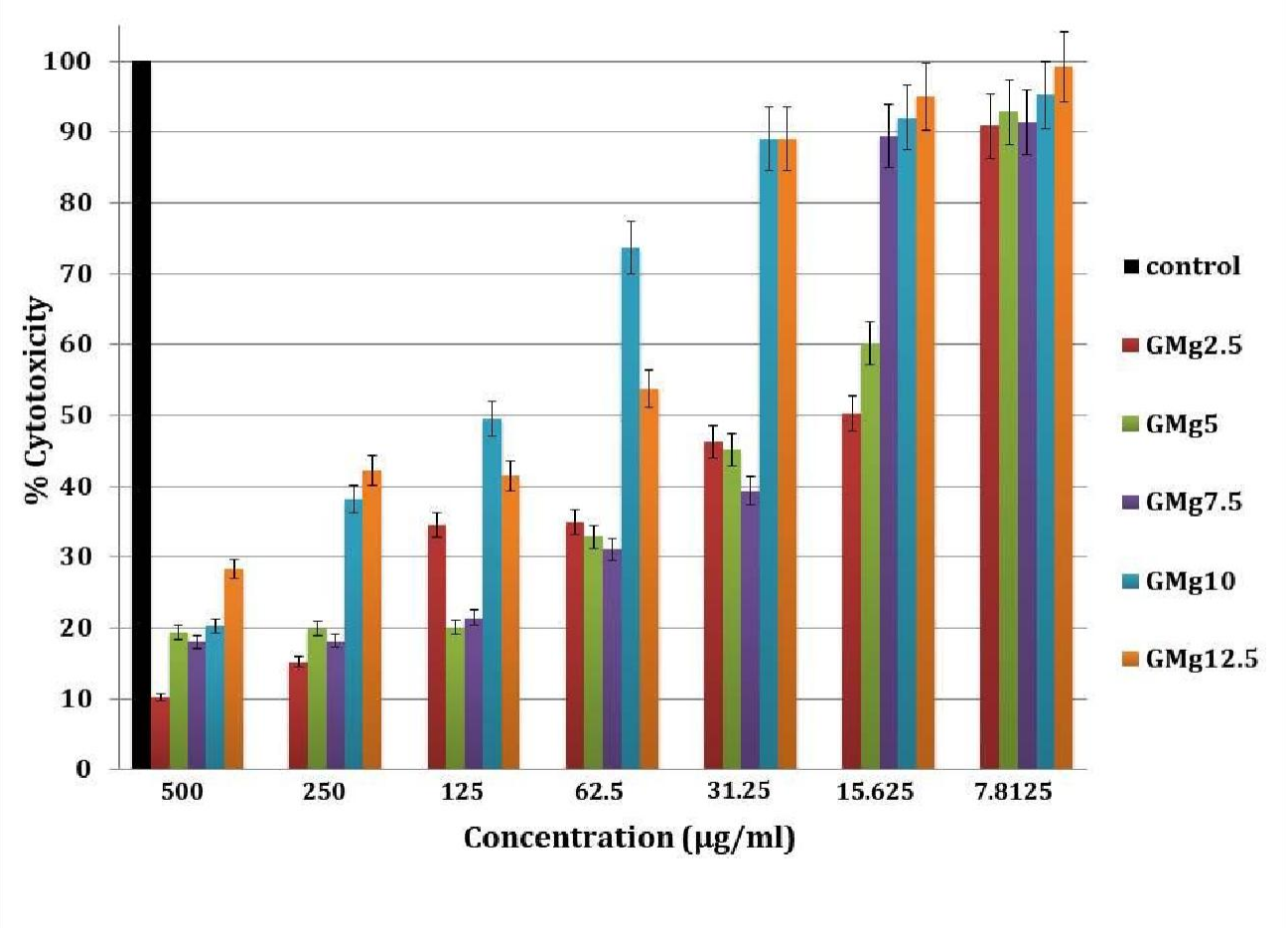

Fig 4.15 MTS cytotoxicity assay results for as prepared MBGs at different concentrations for MG63 human osteosarcoma cell culture.

The cytotoxicity assay for different concentration of all sol-gel glasses for human osteosarcoma cell line MG63 is shown in fig.4.15. The results showed that all the glass samples exhibit non-toxic behaviour at low concentrations. Starting from the concentration of 500 to 7.8125 µg/ml, upto 62.5 µg/ml of concentration all the glass samples are toxic as shown in the fig 4.15. At concentration of 31.25 µg/ml, sample GMg10 and GMg12.5 showed non toxic behaviour while other samples GMg2.5, GMg5 and GMg7.5 are not in the acceptable regime. At concentration 15.625 µg/ml sample GMg7.5, GMg10, GMg12.5 showed complete non toxic behavior while other two samples are not in the acceptable range. Then as the concentration of glass is further reduced upto 7.8125 µg/ml all the glass samples are non toxic and approximately shows similar cytotoxicity. It can also be seen that the sample having higher magnesium content shows non-toxic behavior among all the samples. Thakur et al.[8] obtained non-toxic behaviour of MBGs at

a concentration 0.03 μg/ml, implying that the glass samples show non-toxic behaviour at low concentrations. Thus it can be concluded from the given result that all the samples showed non toxic behavior at low concentrations. i.e. < 7.8125 μg/ml.

REFERENCES

[1] Kaur G, Pickrell G, Sriranganathan N, Kumar V, Homa D. Review and the state of art: Sol-gel and melt quenched bioactive glasses for tissue engineering. *J Biomed Mater Res A* **2016,** 104, 1248- 1275.

[2] Regi MV, Izquierdo- Barba I, Calilla M. Review: Structure and functionalization of mesoporous bioceramics for bone tissue regeneration and local drug delivery. *Phil Trans R Soc Lond A* **2001,** 370, 1400-1421.

[3] Kaur G, Pandey OP, Singh K, Chudasama B, Kumar V. Combined and individual doxorubic/vancomycin drug loading, release kinetics and apatite formation for CaO-CuO-P_2O_5-SiO_2-B_2O_3 mesoporous glasses. *RSC Adv* **2016,** 6, 51046-51056.

[4] Garg S, Thakur S, Gupta A, Kaur G, Pandey OP. Antibacterial and anticancerous drug loading kinetics for (10-x)Cu-xZnO-20CaO-60SiO_2-10P_2O_5($2\leq x\leq 8$) mesoporous bioactive glasses**.** *J Mater Sci: Mater Med* **2017,** 28, 1-14.

[5] Kaur G, Pickrell G, Kimsawatde G, Homa D, Allbee HA, Sriranganathan N. Synthesis, cytotoxicity and hydroxyapatite formation in 27- Tris-SBF for sol-gel based CaO-P_2O_5-SiO_2- B_2O_3-ZnO bioactive glasses. *Biomed Engg* **2014**, 4, 1-14.

[6] Ranjan A, Pothayee N, Seleem MN, Tyler RD, Brenseke B, Sriranganathan N, Riffle JS, Kasimanickam R. Antibacterial efficacy of core-shell nanostructures encapsulating gentamicin against an in ,vivo intracellular Salmonella model. *Int. J. Nanomed* **2009**, 4, 289–297.

[7] Oudadesse H, Dietrich E, Gal YL, Pellen P, Bureau B, Mostafa AA, cathelineau G. Apatite forming ability and cytocompatibility of pure and Zn doped bioactive glasses. *Biomed. Mater*. **2011**, 6, 035006–15.

[8] Thakur S, Garg S, Kaur G, Pandey OP. Effect of Strontium substitution on the Cytocompatibility and 3-D Scaffold Structure for the xSrO-(10-x)MgO-60SiO_2-20CaO-10P_2O_5($2\leq x\leq 8$) Sol-gel glasses. *J Mater Sci: Mater Med* **2017,** 28:89, DOI 10.1007/s10856-017-5901-z

CHAPTER 5

FUTURE ASPECTS

Our studies suggest that mesoporous materials or glasses are recognized as being highly beneficial for loading of drugs and releasing them. In this work, drug has been encapsulated solely into the glasses in order to combat bacterial infections. Since both bacterial infection and bone disease could adversely affect the success of a tissue engineering approach, it is essential to develop MBGs capable of loading and releasing large amount of drugs so as to combat both bacterial infection and bone disease. One of the challenges that we face in loading and releasing the drug is that release of drug from the carrier is not predicted. MBGs are being attractive materials for the loading and releasing of drugs by various research groups. MBGs provides promising properties for their use in drug delivery system as they are biocompatible, highly ordered porous materials, high pore volume and high surface area and many more properties. Future studies are based on the fabrication of bioactive mesoporous materials and their use as drug carriers in drug delivery system. This study can save people from various side effects caused by different types of medicines and therapies that patients go through during illness.